# A Novel Role for PA28gamma-Proteasome in Nuclear Speckle Organization and SR Protein Trafficking.

Véronique Baldin, Muriel Militello, Yann Thomas, Christine Doucet, Weronika Fic, Stephanie Boireau, Isabelle Jariel-Encontre, Marc Piechaczyk, Edouard Bertrand, Jamal Tazi, et al.

# A novel role for PA28γ-proteasome in nuclear speckle organization and SR protein trafficking

Véronique Baldin[*], Muriel Militello[*], Yann Thomas[*], Christine Doucet[*], Weronika Fic[†], Stephanie Boireau[†], Isabelle Jariel-Encontre[†], Marc Piechaczyk[†], Edouard Bertrand[†], Jamal Tazi[†] and Olivier Coux[* §]

Address: [*]Centre de Recherche de Biochimie Macromoléculaire (CRBM-CNRS UMR5237), IFR122, Universités Montpellier 1 et 2, Montpellier, France and [†]Institut de Génétique Moléculaire de Montpellier, (IGMM-CNRS UMR 5535), IFR122, Universités Montpellier 1 et 2, Montpellier, France

Keywords: 20S proteasome, PA28gamma, subnuclear localization, nuclear speckles

Running Head : 20S-PA28γ complexes and nuclear speckles

[§]Corresponding author : Olivier Coux, CRBM-CNRS, 1919 Route de Mende, 34293 Montpellier cedex 5, France

Phone : 33 4 67 61 33 49, Fax : 33 4 67 52 15 59

E-mail : olivier.coux@crbm.cnrs.fr

**Abstract**

**In eukaryotic cells, proteasomes play an essential role in intracellular proteolysis and are involved in the control of most biological processes through regulated degradation of key proteins. Analysis of 20S proteasome localization in human cell lines, using ectopic expression of its CFP-tagged α7 subunit, revealed the presence in nuclear foci of a specific and proteolytically active complex made by association of the 20S proteasome with its PA28γ regulator. Identification of these foci as the nuclear speckles (NS), which are dynamic subnuclear structures enriched in splicing factors (including the SR protein family), prompted us to analyze the role(s) of proteasome-PA28γ complexes in the NS. Here, we show that knockdown of these complexes by small interfering RNAs directed against PA28γ strongly impacts the organization of the NS. Further analysis of PA28γ-depleted cells demonstrated an alteration of intranuclear trafficking of SR proteins. Thus, our data identify proteasome-PA28γ complexes as a novel regulator of NS organization and function, acting most likely through selective proteolysis. These results constitute the first demonstration of a role of a specific proteasome complex in a defined subnuclear compartment, and suggest that proteolysis plays important functions in the precise control of splicing factors trafficking within the nucleus.**

## Introduction

Proteasomes are large proteolytic complexes that play a central role in intracellular proteolysis and are particularly important for the tightly controlled degradation of many critical regulatory proteins (Ciechanover and Schwartz, 2004). The term proteasomes defines a family of complexes, which share a common proteolytic core (the 20S proteasome) but differ in the regulators associated with the complex (Demartino and Slaughter, 1993; Rechsteiner and Hill, 2005). This diversity of proteasome complexes might reflect the necessity for the cell to degrade hundreds of different proteins at the same time, often in a highly selective and regulated manner, and in certain cases only at precise locations in the cell (Pines and Lindon, 2005). However, whether the activity of each of these complexes is restricted to a particular set of substrates or to particular cellular domains is presently unclear.

The 20S proteasome is a cylindrical-shaped protein complex, comprising 28 subunits arranged in four stacked rings: two outer rings each made of seven alpha-type subunits (α1 to α7) and two inner rings each made of seven beta-type subunits (β1 to β7). The catalytic sites are enclosed in the inner catalytic chamber made by the β-type subunits (Groll *et al.*, 1997). In cells, the 20S proteasome is found associated with a variety of regulators that modulate its functions. The best understood 20S regulator is the 19S complex, which binds in an ATP-dependent manner to both ends of the 20S cylinder to form the 26S proteasome that is, in particular, involved in the degradation of ubiquitylated proteins (Coux *et al.*, 1996; Voges *et al.*, 1999). The 20S proteasome can also associate with a variety of other regulators (DeMartino and Slaughter, 1999), including PA200 (Ortega *et al.*, 2005) and the complexes of the PA28 family, PA28α/β and PA28γ (Rechsteiner and Hill, 2005), to form other proteolytic complexes that likely carry out specific functions. PA28α/β is a heptamer of the two closely related PA28α and PA28β subunits (Whitby *et al.*, 2000). It can bind to both ends of 20S proteasome (Gray *et al.*, 1994), and also be integrated into "hybrid proteasomes" in which one molecule of 19S complex and one molecule of PA28α/β are bound at each end of 20S proteasome (Cascio *et al.*, 2002). PA28α/β is essentially cytoplasmic and, *in vitro*, has been shown to stimulate the peptidase, but not the protease, activities of the 20S proteasome (Ma *et al.*, 1992). It is thought to play an important role in the production of MHC class I antigenic peptides (Groettrup *et al.*, 1996). PA28γ, initially called "Ki antigen", is similar to PA28α and β (Kandil *et al.*, 1997; Tanahashi *et al.*, 1997), but forms only

homoheptamers and is mostly nuclear. Its functions are poorly characterized, but studies in mice (Murata *et al.*, 1999; Barton *et al.*, 2004) and flies (Masson *et al.*, 2003) suggest a role for this complex in cell cycle progression and apoptosis. Furthermore, PA28γ has been recently identified as a key player in the degradation of the oncogene SRC-3 (Li *et al.*, 2006) and of the CKI p21 (Chen *et al.*, 2007; Li *et al.*, 2007), and was shown to act as a novel regulator of Cajal Bodies integrity under genotoxic stress (Cioce *et al.*, 2006).

To better understand the specific functions of the various proteasome complexes, it is important to know where in the cells each type of complex is present and active. However, in most previous studies of proteasome localization, only immunofluorescence analyses of the 20S proteasome have been conducted, and it was not known whether the fluorescence corresponded to free 20S or 20S bound to the 19S complex (i.e. the 26S proteasome), or to other regulators. In general, the 20S proteasome appears distributed in both cytoplasmic and nuclear compartments (Reits *et al.*, 1997; Wojcik and DeMartino, 2003), and most of it is found in the soluble fraction after cell lysis. A small percentage, however, seems to be associated with defined cellular structures. In the cytoplasm, the 20S proteasome is found associated with the cytoskeleton (Grossi de Sa *et al.*, 1988), the endoplasmic reticulum (Brooks *et al.*, 2000) and with a perinuclear structure that coincides with the centrosome (Wigley *et al.*, 1999). In the nucleus, the 20S proteasome is found in distinct nuclear regions, including PML bodies (Rockel and von Mikecz, 2002; Wojcik and DeMartino, 2003) and nuclear speckles (Rockel and von Mikecz, 2002; Rockel *et al.*, 2005).

Nuclear speckles (NS), also called interchromatin granule clusters (IGCs), correspond to subnuclear domains enriched in components of the pre-messenger RNA splicing machinery such as the SR protein family (Misteli *et al.*, 1997; Rockel and von Mikecz, 2002; Lamond and Spector, 2003; Rockel *et al.*, 2005). They are highly dynamic domains with a constant in/out shuttling of splicing factors that undergo post-translational modifications (particularly phosphorylation/dephosphorylation) necessary for their subsequent recruitment at transcription sites (Misteli *et al.*, 1998). Indeed, disassembly of NS leads to dramatic reduction of accumulation of splicing factors at transcription sites and perturbs coordination between transcription and splicing (Sacco-Bubulya and Spector, 2002). The presence of proteasomes in NS, together with the fact that proteasome inhibitors promote the accumulation of SR protein SC35 in NS (Rockel and von Mikecz, 2002), suggests that, as with phosphorylation, proteolysis

might be intrinsically involved in the control of the intranuclear trafficking of splicing factors and their repartition between NS and transcription sites.

In this study, we show that a specific form of proteasomes (i.e. 20S proteasome-PA28γ complexes) is present in the NS in an active form. Also, we demonstrate that a reduction of PA28γ expression by siRNA triggers a profound alteration of nuclear speckles organization and affects the recruitment of SR proteins to transcription sites

## Materials and Methods

*Antibodies and compounds*

Antibodies against GFP were obtained from Roche Diagnostic. Antibodies against α3 (PW8115), α4 (PW8120), α6 (PW8100), α7 (PW8110), Mss1/Rpt1 (PW8825) Sug1/Rpt6 (PW9265), PA28γ (PW8190) and PA28β (PW8280) were purchased from Affiniti Research Products Ltd., and antibodies against SC35 (S4045), SF2/ASF (32-4500) and HA (12CA5) were purchased from Sigma, Zymed and Roche Diagnostic, respectively. Alexa and HRP-conjugated secondary antibodies were purchased respectively from Interchim and BioRad SA. Suc-Leu-Leu-Val-Tyr-7amido-4-methylcoumarin (suc-LLVY-AMC, Bachem Biochimie SARL), MG132 (Boston Biochem), DRB (Sigma) and Actinomycin D (Sigma) were dissolved in DMSO. DQ-Ovalbumin was purchased from Calbiochem.

*Plasmid constructs and siRNA*

Human cDNA (768 bp) encoding the full-length α7, with or without the final stop codon, was amplified from a human fibroblast cDNA library by PCR and inserted into $pcDNA_3$ or pML1-ECFP vectors and verified by sequencing. The cDNA coding for α7-ECFP and ECFP were then inserted into pTRE2 vector (Clontech). The pEGFP-hSC35, $pcDNA_3$-Tat and pEGFP-SF2/ASF constructs were generated in the laboratory of J. Tazi and E. Bertrand, respectively. To construct mammalian expression vectors for BiFC analyses, sequences encoding amino acids 1-154 of Enhanced Yellow Fluorescent Protein (EYFP) (N-terminal fragment [YN]) and amino acids 155-239 of EYFP (C-terminal fragment of YFP [YC]) were cloned into $pcDNA_3$. Full-length α7 cDNA (without the final stop) was inserted in $pcDNA_3$-YN and full-length PA28γ cDNA in $pcDNA_3$-YC to create α7-NY and CY-PA28γ fusion proteins, respectively. siRNA duplexes against human PA28γ were purchased from Ambion (PSME3, ID#: 138669) (siRNA#1) or MWG (siRNA#2) (Cioce *et al.*, 2006). Scrambled duplexes (Silencer™ negative control#1) were purchased from Ambion. A PA28γ construct resistant to the siRNA #2 was made by mutation of six nucleotides in PA28γ cDNA subcloned in $pcDNA_3$-3HA vector.

*Cell culture and transfection*

HeLa cells (ATCC), $U_2OS$-tTA (Theis-Febvre *et al.*, 2003), 2E11 cell line (Boireau *et al.*, 2007; du Chéné *et al.*, 2007) and MelJuso cell line expressing constitutively the LMP2-GFP fusion

protein (Reits *et al.*, 1997) were cultured as described in the respective papers. $U_2OS$-tTA cells expressing stably α7-CFP or CFP were established as described (Theis-Febvre *et al.*, 2003). Plasmid transfections in cells were carried out using the JetPEI™ reagent (Qbiogene). 25 nanomoles/ml of each siRNA were transfected into cells with the oligofectamine reagent (Invitrogen), following manufacturer's instructions.

*Immunoprecipitation and immunoblot analysis*

Cells were lysed for 15 min at 4°C in lysis buffer (50 mM Tris pH-HCl 8.0, 5 mM $MgCl_2$, 0.5 mM EDTA, 1 mM ATP, 1 mM DTT, 10% glycerol, 0.5% IGEPAL CA630). This treatment does not solubilize NS components (not shown), which can be later solubilized using a buffer containing 0.3% Triton X-100. Lysates were clarified by centrifugation for 10 min at 10,000 x *g*, and the protein concentration of the supernatant was determined using BSA as a standard (Bradford reagent assay, Pierce). Total lysate (200 μg) was pre-cleared for 30 min and immunoprecipitations were performed using 3 μl of indicated antibodies and Protein A or G magnetic beads (Dynal) in lysis buffer containing 100 mM NaCl. After several washes, bead pellets were boiled in SDS sample buffer, separated by SDS-PAGE and transferred to nitrocellulose membranes. Immunoblotting was performed as described previously (Baldin *et al.*, 1993). Visualization was performed by enhanced chemiluminescence (Perkin Elmer).

*Proteasome activity assay*

Proteasome activity was measured on beads of immunopurified proteasome by incubation at 37°C for 20 min in 100 μl of activity buffer (20 mM Tris-HCl pH 7.5, 5 mM $MgCl_2$, 1 mM ATP, 1 mM DTT, 10 % Glycerol) containing 100 μM suc-LLVY-AMC. The fluorescence of the free AMC generated by proteasome activity ($\lambda_{ex}$= 380 nm, $\lambda_{em}$= 440 nm) was measured on a spectrofluorimeter (Perkin Elmer). Proteasome activity in living cells was analyzed in $U_2OS$ cells as described (Rockel *et al.*, 2005).

*Indirect immunofluorescence*

Cells were transfected or not with expression vectors encoding the mentioned cDNAs. At indicated times after the transfection and/or induction, cells were fixed using 3.7% formaldehyde, then permeabilized with 0.25% Triton–X100 and cold methanol. Proteasome subunits were detected by incubating the cells with the first antibody, followed by a second incubation with

Alexa-594 or 488 conjugated goat anti-mouse (or anti-rabbit) antibody (1:1000) (Molecular Probes). In all cases, DNA was stained with DAPI dye (Sigma). *In situ* hybridization was performed as described (Verheggen *et al*., 2002). Microscopic examinations were performed with a 63X/1.32 NA or 100X/1.4 NA oil immersion objective lens under a Leica DMRA microscope and a 12-bit Micromax YHS 1300 camera. Images were acquired as TIF files using the MetaMorph 6.2 imaging software.

*Fluorescence recovery after photobleaching*

FRAP analyses were performed at 37°C on HeLa cells transiently expressing α7-GFP with a laser scanning microscope (Zeiss LSM Meta 510). The argon laser spectral line (wavelength of 488 nm) was set to an intensity not greater than 0.3% of its total power (458,477,488,514, 30 mW) for image collection. A 40X/1.2 NA water immersion objective was used. After 12 prebleach scans (1 scan/s), a region of interest (ROI) was photobleached using 15 iterations at 3 mW laser power. 12-bit images were collected before, immediately after, and at defined intervals after bleaching (once every 0.8 second). Our total experiment time was set to 130 s., which was sufficient for complete recovery from photobleaching. The mobile fraction (R) was determined using the formula: $R = (F\infty - F0)/(Fi-F0)$. $\tau_{1/2}$ was directly read off of the graph as the time when fluorescence had recovered by 50%.

*RT-PCR*

Total RNA was extracted using the Mini RNA isolation II kit (ZYMO Research). 1 μg of RNA was reverse-transcribed using the first-strand cDNA synthesis kit (GE Healthcare) according to the supplier specifications. cDNAs were amplified with the Taq polymerase (Invitrogen) using specific primers corresponding to S26 and artificial gene mRNA (100 and 193 nucleotides, respectively).

## Results

### *Ectopically expressed proteasome α7 subunit accumulates into nuclear foci*

To study the subcellular localization of the 20S proteasome in living cells, and to avoid overproduction of the protein by transient expression, we established stable $U_2$OS-tTA cell lines expressing 20S α-subunits in fusion with CFP, under an inducible promotor (tet-off). In the tested cell lines, exogenous α-CFPs were expressed at a level similar to that of endogenous α proteins (Figure 1A) (α7-CFP as an example). Surprisingly, in addition to the relatively even cytoplasmic and nuclear distribution of α7 detected by indirect immunofluorescence in parental $U_2$OS-tTA cells, distinct nuclear foci were apparent in α7-CFP expressing cells (Figure 1B) (compare panel endogenous α7 to panel ectopic α7-CFP), which contrasted with the images obtained with cell lines expressing other tagged subunits such as α3-CFP (not shown) or LMP2 (Reits *et al*., 1997). Importantly, despite the apparent brightness of the α7-CFP containing foci, quantification of the fluorescence using the Metamorph software showed that α7-CFP containing foci represent only 7.7% of the total cellular α7-CFP and 22% of the nuclear α7-CFP.

Although this peculiar distribution could reflect the presence of aggregates accumulating upon expression of the CFP-tagged subunit, several lines of evidence indicated that this was not the case. Firstly, we observed that this effect was independent of the presence of the CFP moiety on the subunit: expression of unmodified α7 protein also gave rise to accumulation of the subunit into similar nuclear foci (Figure 1B, right panel). Secondly, upon prolonged induction of the α7-CFP protein, no defect on cell cycle progression could be detected (data not shown), as it would be expected if proteasome function was altered. Thirdly, we observed that the distribution of α7-CFP dramatically changed during mitosis: α7-CFP diffused throughout the cell during metaphase and reformed foci in telophase (Figure S1). In addition, gel filtration analysis of extracts from U2OS-α7-CFP cells revealed the presence of α7-CFP protein only in fractions containing proteasomes (data not shown). Altogether, these experiments indicate that α7-CFP-containing nuclear foci are not aggregates. Furthermore, FRAP (Fluorescence Recovery After Photobleaching) (White and Stelzer, 1999) analysis of the mobility of α7-GFP showed that, after laser-photobleaching of α7-GFP nuclear foci, the mobile fraction of α7-GFP corresponded to 77% (+/- 2.9%) of the protein present in the foci, and that the half time ($\tau_{1/2}$) of complete α7-GFP recovery in the bleached area was 5.75 s (+/- 1.43). This recovery rate is considerably slower than

that of GFP alone ($\tau_{1/2}$ = 0.3 s, see Kruhlak *et al.*, 2000), but equivalent to that of many other mobile nuclear proteins, including transcription factors and RNA splicing components such as SR proteins ($\tau_{1/2}$ = 3-6 s (Phair and Misteli, 2000)), showing that α7-CFP localization into nuclear foci is in fact dynamic.

Biochemical experiments indicated that α7-CFP was readily incorporated into proteasomal complexes (Figure 2). Immunoprecipitation on whole cell extracts demonstrated the presence of other 20S proteasome subunits (α6 subunit) as well as 19S complex subunits (Sug1 protein, an ATPase of this complex) in anti-GFP immunoprecipitates and showed that α7-CFP is also present in anti-Sug1 immunoprecipitates (Figure 2A). The immunoprecipitated CFP-containing complexes were proteolytically active when tested against the proteasome substrate suc-LLVY-AMC (Figure 2B, right panel). Morever, using an *in situ* proteasome-dependent proteolysis assay (Rockel *et al.*, 2005), based on the microinjection of a fluorogenic substrate (DQ-ovalbumin (DQ-OVA) into the cell nucleus, we demonstrated that α7-CFP complexes were active in the nuclear foci. After microinjection of DQ-OVA in parental $U_2OS$ cell nuclei, we confirmed that its degradation (monitored by the appearance of fluorescence) occurs throughout the nucleoplasm but also in discrete foci, as previously published (Rockel *et al.*, 2005) (Figure 2C, upper panel). However, in $U_2OS$ cells expressing ectopic α7, the fluorescent foci resulting from DQ-OVA degradation colocalized completely, in number and shape, with α7 positive nuclear foci (Figure 2C, lower panel). Based on these observations, it can be concluded that the proteasomes complexes containing α7-CFP protein are active in protein degradation.

Finally, we found that whole 20S proteasomes were present in α7-CFP containing nuclear foci: indirect immunofluorescence showed that in contrast to the diffuse nuclear localization observed in $U_2OS$ parental cells (Figure 3A), other tested 20S subunits, namely α4 and α6, localized into the same nuclear foci upon α7 expression (Figure 3B), without any significant variations of their cellular level (Figure 3C). Altogether, these data show that ectopic expression of α7 at moderate level entails recruitment to nuclear foci of genuine, active proteasome complexes, and not accumulation of free α7.

***Identification of the nuclear foci as the nuclear speckles***

A critical point was to define the nature of the nuclear foci evidenced by expression of α7-CFP. As previous reports described that 20S proteasomes localized to subnuclear domains such as PML bodies (Rockel and von Mikecz, 2002; Wojcik and DeMartino, 2003) or nuclear speckles (NS) (Chen *et al.*, 2002; Rockel and von Mikecz, 2002), we analyzed by indirect immunofluorescence the potential colocalization of α7-CFP with markers of those two nuclear subdomains, using antibodies raised against PML and SR proteins. Whereas the nuclear foci were clearly distinct from the PML bodies (data not shown), we observed a complete colocalization of α7-CFP with SC35 protein (Figure 4A), a member of the SR protein family that is concentrated in nuclear speckles (Misteli *et al.*, 1997; Lamond and Spector, 2003). To verify that the localization of α7-CFP in NS was not a coincidence, we treated the cells with transcriptional inhibitors (actinomycin D and DRB) that cause NS to enlarge and round up (Spector, 1993) (for a review, see Lamond and Spector, 2003). In these cases, we observed similar morphological changes for the foci labeled by α7-CFP and SC35 (Figure 4B), indicating that proteasome complexes containing α7-CFP and NS are tightly connected.

***20S proteasome-PA28γ complexes, but not 26S proteasome complexes, are recruited to NS upon α7 expression***

To determine to which regulator(s) the 20S proteasome was associated with in the NS, we performed indirect immunofluorescence analyses using specific antibodies raised against components of different regulatory complexes. Whereas colocalization of α7-CFP and two ATPases (Mss1 and Sug1) of the 19S regulator of the 20S proteasome could be detected in both the cytoplasm and the nucleus of the cells, these ATPases did not accumulate together with α7-CFP into the NS, unlike the α4 subunit of the 20S proteasome (Figures 5A and S2A and B). These results indicate that 26S proteasome is not the proteasomal complex recruited to the NS upon α7 ectopic expression. We thus tested for the presence of other regulators of the 20S proteasome. Strikingly, in $U_2OS$ cells expressing α7-CFP, PA28γ accumulated with α7 (and thus with 20S proteasomes) in these foci (Figures 5B and S2A and B), whereas, in contrast, the related regulator PA28α/β did not (Figure 5A, lower panel). We also noted that, during mitosis, when the foci reversibly redistribute throughout the cell, the localization of PA28γ strictly followed that of α7-CFP containing 20S proteasome (Figure S1).

Together, these experiments show that ectopic expression of α7 (-CFP) entails accumulation into the NS of 20S proteasome-PA28γ complexes, which are active in protein degradation (Figure 2C). This accumulation is specific for this type of proteasome complex, since the 19S regulatory complex of the 20S proteasome, visualized here by following its Sug1 and Mss1 subunits, is not recruited in the NS, even though α7-CFP-containing 20S proteasomes can associate to the 19S complex elsewhere in the cells, as shown by co-immunoprecipitation experiments (Figure 2A and B).

We confirmed the interaction between α7-CFP-containing 20S proteasome and PA28γ in cell extracts by co-immunoprecipitation from mildly solubilized (S1 fraction, no extraction of α7-CFP nuclear foci) or triton-solubilized cell extracts (S2 fraction, obtained after solubilization of α7-CFP nuclear foci) using antibodies directed against either α7, GFP or PA28γ (Figure 6A). Even though the majority of 20S proteasome-PA28γ complexes was present in the S1 fraction, the complexes were also present in the S2 fraction enriched in NS (Figure 6A), and were active when tested for degradation of the proteasomal peptide substrate Suc-LLVY-AMC (data not shown). Notably, the distribution of the complexes between the S1 and S2 fractions is in agreement with the low percentage of α7-CFP present in the nuclear foci, estimated by fluorescence quantification (see above). We then used the Bimolecular Fluorescence Complementation (BiFC) technique to evaluate directly, *in cellulo,* the ability of α7 to interact with PA28γ in the NS. This technique is based on the fact that the YFP chromophore can be reconstituted in cells when two chimeric proteins, each harboring half of the chromophore, interact (Kerppola, 2006). When α7 fused to the C-terminal half of YFP (α7-CY) was coexpressed in cells with PA28γ fused to the N-terminal half of YFP (NY-PA28γ), the fluorescence could be reconstituted throughout the nuclei, with a marked accumulation in nuclear foci, which most likely correspond to NS (Figure 6B). Interaction was also observed in the nucleus between molecules of PA28γ, as expected since PA28γ forms heptamers, and curiously between molecules of α7 as well (Figure 6B) (see discussion). Together, these results confirm the *in cellulo* interaction between 20S proteasome and its PA28γ regulator and strongly suggest that 20S proteasome-PA28γ complexes are indeed present in the NS.

***PA28γ is present in the nuclear speckles without expression of α7-CFP***

To exclude the possibility that the localization of 20S-PA28γ complexes in the NS was only due to α7 ectopic expression, we examined the localization of PA28γ in parental $U_2OS$ cells. Since in fixed cells no clear specific intra-nuclear localization of PA28γ could be detected, soluble PA28γ was removed by simultaneous fixation and permeabilization of the cells. Under these conditions, we clearly visualized the colocalization of the remaining endogenous PA28γ with SC35 protein in the NS (Figure 7A). Therefore, 20S-PA28γ complexes are present in the NS without α7 ectopic expression, although their NS localization is strongly enhanced by it. Curiously, we were unable to detect the endogenous 20S proteasome in the NS, even when different conditions of permeabilization and various antibodies were used, although these complexes have been seen previously by others in the NS (Rockel and von Mikecz, 2002; Rockel *et al.*, 2005). However, we could vizualize a physical interaction between 20S proteasome and SR proteins in co-immunoprecipitation experiments using extracts from cells expressing α7 and SF2/ASF-GFP proteins (Figure 7B). By contrast, SF2/ASF was not detected in anti-PA28γ immunoprecipitates, possibly because the PA28γ epitope was masked by the interaction with SF2/ASF-GFP.

***Roles of 20S proteasome-PA28γ complexes in the structural integrity of the NS***

The results described above demonstrate for the first time that 20S proteasome-PA28γ complexes are present in the NS and suggest a specific role of these complexes in this subnuclear domain. To gain insight into this role, we investigated the effect of the absence of 20S-PA28γ complexes, using siRNA duplexes directed against PA28γ. Because the complete absence of PA28γ appeared to be toxic to our cells, we could only analyze a partial knockdown of PA28γ (decreased approximately 70% from its normal level) (Figure 8A). Very interestingly, we observed that in cells treated with PA28γ–siRNA, but not in control cells, α7-CFP nuclear foci were fewer and appeared significantly larger and less dot-like compared to untreated cells (Figures 8B (upper panels) and 8C). Furthermore, when the distribution of either endogenous SC35 (Figures 8B and 8D) and SF2/ASF (Figure 8E), or exogenous SF2/ASF-GFP (Figure 11A), was analyzed by immunofluorescence, the same structural alteration of the NS was observed, showing that not only the distribution of the proteasome, but that of the entire NS population was affected by PA28γ knockdown. Importantly, ectopic expression of α7 was not required for these effects, since the same alteration of the NS was observed in parental $U_2OS$ cells (Figure 8F) upon PA28γ

knockdown. Moreover, the same results were obtained using a second siRNA duplex (siRNA# 2) (Figure 9A and B), directed against another PA28γ mRNA region and already validated in a previous study (Cioce *et al*., 2006). Importantly, the effect of this siRNA was reversed by co-expression of a construct resistant to the siRNA (Figure 9B). Therefore, alteration of the NS is clearly due to PA28γ depletion, showing that endogenous 20S-PA28γ complexes are necessary for typical NS organization in $U_2OS$ cells.

To test whether the effect of PA28γ knockdown was restricted to the NS, we analyzed by indirect immunofluorescence the organization of other known nuclear domains such as PML bodies and Cajal Bodies (CB) (Figure 10). In cells treated with PA28γ–siRNA, no changes were observed in PML bodies (Figure 10B) or in the number and appearance of CBs detected by anti-TGS1 (TrimethylGuanosine Synthase) or anti-SMN antibodies (Figure 10A, upper panels). However, we noticed a redistribution of coilin (an autoantigen marker of CBs). In cells knocked down for PA28γ, coilin was still present in the CBs, but appeared additionally in other nuclear regions (Figure 10A, lower panel). Most likely, the partial delocalization of coilin was due to the fact that PA28γ plays a role in its nuclear distribution (Cioce *et al*., 2006). Altogether, our results suggest that PA28γ knockdown does not alter the whole nuclear organization but impacts mostly NS integrity, even though it is clear that PA28γ must have functions outside the NS.

NS are known to be highly dynamic structures in which splicing factors undergo post-translational modifications (particularly phosphorylations) that are required for the SR proteins to leave the NS and be subsequently recruited at transcription sites (Misteli *et al*., 1998). We thus tested whether knockdown of PA28γ altered the capacity of SR proteins to be recruited at a specific transcription site. For this purpose, we used the 2E11 (also called pU2OS_Exo1) cell line, a derivated $U_2OS$ cell line that harbors an integrated inducible HIV-1 reporter gene containing a splice site for SF2/ASF. An additional RNA tag (MS2) was inserted to facilitate its visualization by *in situ* hybridization (Boireau *et al*., 2007; du Chéné *et al*., 2007). The ability of SF2/ASF to be recruited to nascent pre-mRNAs was estimated by measuring the relative level of the protein at the transcription site (TS, visualized as a nuclear dot by *in situ* hybridization with a MS2-Cy3 probe) compared to its level at a neighboring NS (Figures 11A and S3). To eliminate the variation of GFP level, due to transfection efficiency, only loci of cells presenting a similar level of SF2/ASF-GFP in NS were scored. Results were summarized in the histogram shown in

Figure 11B. In untreated cells or with control-siRNA treatment, the level of SF2/ASF-GFP at the TS was generally higher than in the NS, reflecting the normal recruitment of SF2/ASF-GFP to TS. In contrast, with PA28γ-siRNA treatment, the level of SF2/ASF-GFP at the TS was most of the time lower than at the NS without affecting the transcription level of the artificial gene (Figure 11C). These results show that under PA28γ-siRNA treatment, the recruitment of SR proteins to the active TS is largely reduced, although not abolished.

Together, these experiments demonstrate that 20S proteasme-PA28γ complexes play an important role in NS organization and dynamics and mediate a process involved in the regulation of accumulation and/or targeting of splicing factors to transcription sites.

**Discussion**

We show here that active 20S proteasome-PA28γ complexes are present in the NS, and that reduction of PA28γ levels, using siRNA, dramatically alters NS organization and nuclear trafficking of splicing factors. Our data thus demonstrate a new role of 20S-PA28γ complexes in nuclear organization, and provide novel important information for our understanding of both the specific functions and localization of the various forms of proteasomes and the regulation of NS structure and dynamics.

Our discovery originates from the serendipitous observation that ectopic expression of the proteasomal α7 subunit triggers accumulation of 20S proteasome-PA28γ complexes in the NS. This observation raises the intriguing and puzzling problem of how this effect is mediated. One possibility was that overexpression of α7 led to an increase of the cellular concentration of 20S proteasome, but we found no evidence to support this supposition. One alternative hypothesis is that α7 ectopic expression entails incorporation of more than two α7 subunits into individual 20S proteasome complexes. Indeed, some plasticity in proteasome assembly has been documented in yeast, in which α3 could be replaced by α4 (Velichutina *et al*., 2004). In this respect, it is remarkable that α7 seems to possess a greater propensity to interact to PA28γ than other subunits. When we used the proteasome subunit α3, no interaction with PA28γ could be detected by BiFC, contrary to the result obtained for α7, suggesting that (i) PA28γ does not interact identically with all α subunits of the proteasome and (ii) within the 20S proteasome, the α7 subunit possesses certain sequence and/or structural features that makes it a favored partner for PA28γ. Thus, a proteasome with more than one α7 subunit per α-ring could either have a higher affinity for PA28γ, or impose a particular conformation to the complex formed with PA28γ, two mechanisms that in turn could impact on the steady-state nuclear distribution of the 20S-PA28γ complex.

In any case, even if the exact reasons for accumulation of 20S-PA28γ in NS upon α7 ectopic expression remain to be elucidated, several arguments show that the presence of 20S-PA28γ complexes in the NS is physiologic, albeit not easily detectable normally. In particular, the presence of active 20S proteasome in the NS, as previously documented by others (Rockel *et al*., 2005), together with our results demonstrating that (i) PA28γ can be detected in the NS without ectopic α7 expression, (ii) knockdown of endogenous PA28γ alters NS morphology, and (iii) 20S proteasomes can interact with PA28γ in the NS (as illustrated by colocalization, affinity

purification and *in vivo* interaction (BiFC)), demonstrate that these complexes constitute an important active form of the proteasome in the NS.

Regarding the function(s) of 20S-PA28γ complexes in the NS, it is most likely that these complexes mediate the local degradation of specific proteins, even though they certainly have other substrates in other nuclear regions. We hypothesized that substrates of 20S-PA28γ complexes in the NS could be the SR proteins themselves since it has been reported that the intrinsic NS component SC35 is stabilized by proteasome inhibitors (Rockel and von Mikecz, 2002). However, in our cells, expression of α7-CFP or knockdown of PA28γ did not alter the half-life of SC35 (data not shown). Other attractive substrates for 20S-PA28γ complexes are kinases or phosphatases present in the NS (Colwill *et al.*, 1996; Misteli and Spector, 1996; Wang *et al.*, 1998; Ko *et al.*, 2001). Indeed, these enzymes control the phosphorylation status of SR proteins and thereby their recruitment at transcription sites (Misteli *et al.*, 1998). Thus, alteration of the expression level of one or several of these enzymes could explain the alteration of both the morphology of the NS and the recruitment of SR proteins to transcription sites seen upon PA28γ knockdown. Obviously, to understand the role(s) of 20S-PA28γ complexes in the NS, an important development for the future will be to identify their nuclear substrates, particularly those localized in the NS.

Nevertheless, even without this information, our observations provide additional demonstration that, within the family of proteasome complexes, 20S proteasome-PA28γ complexes have specific functions in the cell nucleus. Until recently, the functions of PA28γ have remained quite elusive. Genetic manipulations in mice and *Drosophila* have suggested that it might be involved in cell cycle progression and have anti-apoptotic functions (Rechsteiner and Hill, 2005). However, its exact role in these processes is not understood. Biochemical analyses have shown that PA28γ can activate peptide degradation by the 20S proteasome *in vitro* (Realini *et al.*, 1997), but it has been demonstrated only recently that PA28γ is indeed involved in the degradation of proteins, namely the HCV (Hepatitis C virus) core protein (Moriishi *et al.*, 2003), the SRC-3 oncogene and the CKI p21 (Li *et al.*, 2006; Chen *et al.*, 2007; Li *et al.*, 2007). PA28γ has also been identified as a novel regulator of Cajal Bodies integrity (Cioce *et al.*, 2006), but it was unclear in this case whether 20S proteasome was required for this process. We now additionally show that 20S-PA28γ complexes are involved in the control of nuclear trafficking of splicing

factors, since reduction of PA28γ levels by siRNA strongly perturbs NS morphology and impairs recruitment of SR proteins (SF2/ASF) at transcription sites. The physiologic importance of this role is presently unclear, since knockdown of PA28γ did not appear to affect transcription (as evaluated by RT-PCR of a specific gene (Figure 11C), or globally by 5-FU incorporation (Figure S4A)), nor to impair globally the specificity of the splicing machinery, since no variations were detected on various endogenous and transfected genes subjected to alternative splicing (Figure S4, B and C). Our results are similar to previously described data (Caceres *et al.*, 1997; Misteli *et al.*, 1998) showing that an SF2/ASF mutant (Δ–RS) was able to perform alternative splicing *in vivo*, in a manner very similar to the wild type, in absence of its recruitment to transcription sites, and suggesting that recruitment to the TS does not always reflect the functional properties of splicing factors. However, one possibility in our case is that the low level of SF2/ASF still present at TS is in fact sufficient for normal splicing.

Another question arising from our data is how 20S-PA28γ complexes are targeted to the NS. Our FRAP analyses demonstrated that α7-GFP (and therefore the proteasome) mobility is high in the NS, indicating that the complexes shuttle into and out of the NS. Currently, the mechanism of the targeting of the complex to the NS is unclear, as neither proteasome subunits nor PA28γ display signature motifs of NS proteins, such as RS domains, for example. Possibly, protein(s) binding to 20S proteasome and/or PA28γ could act as adaptor(s) facilitating the docking of the complex to the NS. Interestingly, since we detected a physical interaction between the 20S proteasome and SF2/ASF, SR proteins themselves could be responsible for targeting proteasomes to the NS.

In conclusion, the data presented here demonstrate that 20S proteasome associated with its PA28γ regulator plays a critical role in the NS since it appears necessary for their structural organization and for intranuclear trafficking of splicing factors. Our data also suggest that the specificity of proteasome-dependent proteolysis, which is often considered as being regulated at the level of the ubiquitylation, can be controlled by complex mechanisms operating at the level of the proteasome and its intracellular localization. Further analysis of the role of 20S proteasome-PA28γ complexes in the NS should provide new information on the mechanisms involved in the control of nuclear organization. Our results highlight a novel layer of complexity in the regulation of NS architecture and function, as well as SR protein trafficking, and suggest that intracellular proteolysis is intrinsically involved in the regulation of nuclear plasticity.

**Acknowledgements** :

We thank E. Reits for MelJuso cells, U. Seifert for PA28γ cDNA and R. Bordonné for antibodies (TGS1 and SMN). We also thank our colleagues for their help, suggestions and criticisms, and the cell imaging facility (Montpellier RIO Imaging) for the quality of its service. This work was supported by a grant from the Association pour la Recherche sur le Cancer to OC (ARC n° 3243), an ACI-BCMS from the French Research Ministry (OC), the European contract n°QLG1-CT-2001-02026 (OC) and a grant to JT from the Agence Nationale de la Recherche (ANR-05-BLAN-0261-01). CD was a recipient of a fellowship from the Fondation de la Recherche Médicale (FRM). EB and MP laboratories are “Equipes labellisées de la Ligue Nationale contre le Cancer”.

**References**


Baldin, V., Lukas, J., Marcote, M.J., Pagano, M., and Draetta, G. (1993). Cyclin D1 is a nuclear protein required for cell cycle progression in G1. Genes Dev *7*, 812-821.

Barton, L.F., Runnels, H.A., Schell, T.D., Cho, Y., Gibbons, R., Tevethia, S.S., Deepe, G.S., Jr., and Monaco, J.J. (2004). Immune Defects in 28-kDa Proteasome Activator gamma-Deficient Mice. J Immunol *172*, 3948-3954.

Boireau, S.*, et al.* (2007). The transcriptional cycle of HIV-1 in real-time and live cells. J Cell Biol *179*, 291-304.

Brooks, P., Murray, R.Z., Mason, G.G., Hendil, K.B., and Rivett, A.J. (2000). Association of immunoproteasomes with the endoplasmic reticulum. Biochem J *352*, 611-615.

Caceres, J.F., Misteli, T., Screaton, G.R., Spector, D.L., and Krainer, A.R. (1997). Role of the modular domains of SR proteins in subnuclear localization and alternative splicing specificity. J Cell Biol *138*, 225-238.

Cascio, P., Call, M., Petre, B.M., Walz, T., and Goldberg, A.L. (2002). Properties of the hybrid form of the 26S proteasome containing both 19S and PA28 complexes. Embo J *21*, 2636-2645.

Chen, M., Rockel, T., Steinweger, G., Hemmerich, P., Risch, J., and Von Mikecz, A. (2002). Subcellular recruitment of fibrillarin to nucleoplasmic proteasomes: implications for processing of a nucleolar autoantigen. Mol Biol Cell *13*, 3576-3587.

Chen, X., Barton, L.F., Chi, Y., Clurman, B.E., and Roberts, J.M. (2007). Ubiquitin-Independent Degradation of Cell-Cycle Inhibitors by the REGgamma Proteasome. Mol Cell *26*, 843-852.

Ciechanover, A., and Schwartz, A.L. (2004). The ubiquitin system: pathogenesis of human diseases and drug targeting. Biochim Biophys Acta *1695*, 3-17.

Cioce, M., Boulon, S., Matera, A.G., and Lamond, A.I. (2006). UV-induced fragmentation of Cajal bodies. J Cell Biol *175*, 401-413.

Colwill, K., Pawson, T., Andrews, B., Prasad, J., Manley, J.L., Bell, J.C., and Duncan, P.I. (1996). The Clk/Sty protein kinase phosphorylates SR splicing factors and regulates their intranuclear distribution. Embo J *15*, 265-275.

Coux, O., Tanaka, K., and Goldberg, A.L. (1996). Structure and Functions of the 20S and 26S Proteasomes. Annu Rev Biochem *65*, 801-847.

Demartino, G.N., and Slaughter, C.A. (1993). Regulatory proteins of the proteasome. Enzyme & Protein *47*, 314-324.

DeMartino, G.N., and Slaughter, C.A. (1999). The Proteasome, a Novel Protease Regulated by Multiple Mechanisms. J Biol Chem *274*, 22123-22126.

du Chéné, I.*, et al.* (2007). Suv39H1 and HP1gamma are responsible for chromatin-mediated HIV-1 transcriptional silencing and post-integration latency. Embo J *26*, 424-435.

Gray, C.W., Slaughter, C.A., and Demartino, G.N. (1994). PA28 activator protein forms regulatory caps on proteasome stacked rings. J Mol Biol *236*, 7-15.

Groettrup, M., Soza, A., Eggers, M., Kuehn, L., Dick, T.P., Schild, H., Rammensee, H.G., Koszinowski, U.H., and Kloetzel, P.M. (1996). A Role For the Proteasome Regulator PA28-Alpha In Antigen Presentation. Nature *381*, 166-168.

Groll, M., Ditzel, L., Lowe, J., Stock, D., Bochtler, M., Bartunik, H.D., and Huber, R. (1997). Structure Of 20S Proteasome From Yeast At 2.4 Å Resolution. Nature *386*, 463-471.

Grossi de Sa, M.F., Martins de Sa, C., Harper, F., Olink- Coux, M., Huesca, M., and Scherrer, K. (1988). The association of prosomes with some of the intermediate filament networks of the animal cell. J Cell Biol *107*, 1517-1530.

Hu, C.D., Chinenov, Y., and Kerppola, T.K. (2002). Visualization of Interactions among bZIP and Rel Family Proteins in Living Cells Using Bimolecular Fluorescence Complementation. Mol Cell *9*, 789-798.

Kandil, E., Kohda, K., Ishibashi, T., Tanaka, K., and Kasahara, M. (1997). Pa28 Subunits Of the Mouse Proteasome - Primary Structures and Chromosomal Localization Of the Genes. Immunogenetics *46*, 337-344.

Kerppola, T.K. (2006). Visualization of molecular interactions by fluorescence complementation. Nat Rev Mol Cell Biol *7*, 449-456.

Ko, T.K., Kelly, E., and Pines, J. (2001). CrkRS: a novel conserved Cdc2-related protein kinase that colocalises with SC35 speckles. J Cell Sci *114*, 2591-2603.

Kruhlak, M.J., Lever, M.A., Fischle, W., Verdin, E., Bazett-Jones, D.P., and Hendzel, M.J. (2000). Reduced mobility of the alternate splicing factor (ASF) through the nucleoplasm and steady state speckle compartments. J Cell Biol *150*, 41-51.

Lamond, A.I., and Spector, D.L. (2003). Nuclear speckles: a model for nuclear organelles. Nat Rev Mol Cell Biol *4*, 605-612.

Li, X., Amazit, L., Long, W., Lonard, D.M., Monaco, J.J., and O'Malley B, W. (2007). Ubiquitin- and ATP-Independent Proteolytic Turnover of p21 by the REGgamma-Proteasome Pathway. Mol Cell *26*, 831-842.

Li, X., Lonard, D.M., Jung, S.Y., Malovannaya, A., Feng, Q., Qin, J., Tsai, S.Y., Tsai, M.J., and O'Malley B, W. (2006). The SRC-3/AIB1 Coactivator Is Degraded in a Ubiquitin- and ATP-Independent Manner by the REGgamma Proteasome. Cell *124*, 381-392.

Ma, C.P., Slaughter, C.A., and DeMartino, G.N. (1992). Identification, purification, and characterization of a protein activator (PA28) of the 20 S proteasome (macropain). J Biol Chem *267*, 10515-10523.

Masson, P., Lundgren, J., and Young, P. (2003). Drosophila Proteasome Regulator REGgamma: Transcriptional Activation by DNA Replication-related Factor DREF and Evidence for a Role in Cell Cycle Progression. J Mol Biol *327*, 1001-1012.

Misteli, T., Caceres, J.F., Clement, J.Q., Krainer, A.R., Wilkinson, M.F., and Spector, D.L. (1998). Serine phosphorylation of SR proteins is required for their recruitment to sites of transcription in vivo. J Cell Biol *143*, 297-307.

Misteli, T., Caceres, J.F., and Spector, D.L. (1997). The dynamics of a pre-mRNA splicing factor in living cells. Nature *387*, 523-527.

Misteli, T., and Spector, D.L. (1996). Serine/threonine phosphatase 1 modulates the subnuclear distribution of pre-mRNA splicing factors. Mol Biol Cell *7*, 1559-1572.

Moriishi, K., *et al*. (2003). Proteasome Activator PA28gamma-Dependent Nuclear Retention and Degradation of Hepatitis C Virus Core Protein. J Virol *77*, 10237-10249.

Murata, S., Kawahara, H., Tohma, S., Yamamoto, K., Kasahara, M., Nabeshima, Y., Tanaka, K., and Chiba, T. (1999). Growth Retardation in Mice Lacking the Proteasome Activator PA28gamma. J Biol Chem *274*, 38211-38215.

Ortega, J., Bernard Heymann, J., Kajava, A.V., Ustrell, V., Rechsteiner, M., and Steven, A.C. (2005). The Axial Channel of the 20S Proteasome Opens Upon Binding of the PA200 Activator. J Mol Biol *346*, 1221-1227.

Phair, R.D., and Misteli, T. (2000). High mobility of proteins in the mammalian cell nucleus. Nature *404*, 604-609.

Pines, J., and Lindon, C. (2005). Proteolysis: anytime, any place, anywhere? Nat Cell Biol *7*, 731-735.

Realini, C., Jensen, C.C., Zhang, Z., Johnston, S.C., Knowlton, J.R., Hill, C.P., and Rechsteiner, M. (1997). Characterization of recombinant REGalpha, REGbeta, and REGgamma proteasome activators. J Biol Chem *272*, 25483-25492.

Rechsteiner, M., and Hill, C.P. (2005). Mobilizing the proteolytic machine: cell biological roles of proteasome activators and inhibitors. Trends Cell Biol *15*, 27-33.

Reits, E.A.J., Benham, A.M., Plougastel, B., Neefjes, J., and Trowsdale, J. (1997). Dynamics of proteasome distribution in living cells. Embo J *16*, 6087-6094.

Rockel, T.D., Stuhlmann, D., and von Mikecz, A. (2005). Proteasomes degrade proteins in focal subdomains of the human cell nucleus. J Cell Sci *118*, 5231-5242.

Rockel, T.D., and von Mikecz, A. (2002). Proteasome-dependent processing of nuclear proteins is correlated with their subnuclear localization. J Struct Biol *140*, 189-199.

Sacco-Bubulya, P., and Spector, D.L. (2002). Disassembly of interchromatin granule clusters alters the coordination of transcription and pre-mRNA splicing. J Cell Biol *156*, 425-436.

Spector, D.L. (1993). Nuclear organization of pre-mRNA processing. Curr Opin Cell Biol *5*, 442-447.

Tanahashi, N., *et al*. (1997). Molecular properties of the proteasome activator PA28 family proteins and gamma-interferon regulation. Genes Cells *2*, 195-211.

Theis-Febvre, N., Filhol, O., Froment, C., Cazales, M., Cochet, C., Monsarrat, B., Ducommun, B., and Baldin, V. (2003). Protein kinase CK2 regulates CDC25B phosphatase activity. Oncogene *22*, 220-232.

Velichutina, I., Connerly, P.L., Arendt, C.S., Li, X., and Hochstrasser, M. (2004). Plasticity in eucaryotic 20S proteasome ring assembly revealed by a subunit deletion in yeast. Embo J *23*, 500-510.

Verheggen, C., Lafontaine, D.L., Samarsky, D., Mouaikel, J., Blanchard, J.M., Bordonne, R., and Bertrand, E. (2002). Mammalian and yeast U3 snoRNPs are matured in specific and related nuclear compartments. Embo J *21*, 2736-2745.

Voges, D., Zwickl, P., and Baumeister, W. (1999). The 26S Proteasome: A Molecular Machine Designed for Controlled Proteolysis. Annu. Rev. Biochem. *68*, 1015-1068.

Wang, H.Y., Lin, W., Dyck, J.A., Yeakley, J.M., Songyang, Z., Cantley, L.C., and Fu, X.D. (1998). SRPK2: a differentially expressed SR protein-specific kinase involved in mediating the interaction and localization of pre-mRNA splicing factors in mammalian cells. J Cell Biol *140*, 737-750.

Whitby, F.G., Masters, E.I., Kramer, L., Knowlton, J.R., Yao, Y., Wang, C.C., and Hill, C.P. (2000). Structural basis for the activation of 20S proteasomes by 11S regulators. Nature *408*, 115-120.

White, J., and Stelzer, E. (1999). Photobleaching GFP reveals protein dynamics inside live cells. Trends Cell Biol *9*, 61-65.

Wigley, W.C., Fabunmi, R.P., Lee, M.G., Marino, C.R., Muallem, S., DeMartino, G.N., and Thomas, P.J. (1999). Dynamic association of proteasomal machinery with the centrosome. J Cell Biol *145*, 481-490.

Wojcik, C., and DeMartino, G.N. (2003). Intracellular localization of proteasomes. Int J Biochem Cell Biol *35*, 579-589.

**Figure legends**

**Figure 1.** Ectopic α7-CFP and α7 accumulate into nuclear foci. (A) Expression of the α7-CFP protein in cells. Total cellular extracts (30 $\mu$g) of human osteosarcoma $U_2OS$-tTA (U), or $U_2OS$-tTA cells stably transfected with vectors conditionally expressing α7-CFP (α7) cultured in the absence of tetracycline for 48 hours, were separated by electrophoresis and analyzed by immunoblotting using anti-α7 antibodies. (B) The cellular distribution of α7 in $U_2OS$-tTA cells either untransfected (endogenous α7), stably transfected with $pTRE_2$-α7-CFP (ectopic α7-CFP), or transiently transfected with $pcDNA_3$-α7 (ectopic α7), was analyzed by indirect immunofluorescence using anti-α7 antibodies (red) or by CFP fluorescence (cyan) on fixed cells. Arrows indicate transiently transfected cells. Observation with a 63X objective. Bar, 10 μm.

**Figure 2.** α7-CFP is incorporated into active proteasome complexes that accumulate in nuclear foci. (A) Total cell lysate from human osteosarcoma $U_2OS$-tTA cells stably transfected with vectors conditionally expressing α7-CFP (α7) or CFP (CFP) cultured in the absence of tetracycline for 48 hours, and from MelJuso cells stably expressing LMP2-GFP (LMP2), were subjected to immunoprecipitation (IP) with anti-GFP or anti-Sug1 antibodies. Immunoprecipitated proteins as well as 30 $\mu$g of $U_2OS$-tTA total extract (T) were separated by electrophoresis and analyzed by immunoblotting using the indicated antibodies. (B) Proteins immunoprecipitated with either anti-Sug1 or anti-GFP antibodies from total cell extracts were tested for proteasomal activity using the peptide suc-LLVY-AMC as a substrate, in the presence (+) or not (-) of 50 $\mu$M MG132 (first bar: no IP in the assay). (C) Proteasomes are active in nuclear foci. $U_2OS$-tTA cells (upper panel) or $U_2OS$-tTA cells transiently expressing α7 (lower panel) were microinjected (24 hours post-transfection) with the fluorogenic substrate protein DQ-OVA (0.5 mg/ml). The substrate was injected into the nuclei. Cells were incubated 10 min at 37°C then fixed and the fluorescent DQ-OVA degradation products were visualized by the appearance of green fluorescence. α7 was detected by indirect immunofluorescence with anti-α7 (red) (63X objective). Bar, 10 μm. $U_2OS$-tTA-α7-CFP cells were not used in this experiment due to the overlap of the fluorescence spectrums of CFP and of DQ-OVA degradation products.

**Figure 3.** Ectopic expression of α7-CFP promotes recruitment of whole 20S proteasomes into the nuclear foci. Parental $U_2OS$-tTA cells (A) and $U_2OS$-tTA-α7-CFP cells induced for 48h for α7-CFP expression (B), were subjected to indirect immunofluorescence using antibodies directed

against the α4 and α6 subunits of the 20S proteasome (red). α7-CFP fusion protein was detected by CFP fluorescence. Wide-field overlay images and enlargements of marked area are shown. All observations were done with a 63X objective. Bar, 10 μm. (C) Expression of α7-CFP does not alter expression level of other 20S proteasome subunits. 30 $\mu$g of total protein extract from $U_2$OS-tTA (U) and induced $U_2$OS-tTA-α7-CFP (α7) cells were separated by electrophoresis and analyzed by immunoblot (IB) using the indicated antibodies.

**Figure 4.** The nuclear foci enriched in 20S proteasome-α7-CFP complexes correspond to the NS. (A) $U_2$OS-tTA-α7-CFP were fixed 48h after α7-CFP induction, permeabilized and stained with a monoclonal antibody directed against the phosphorylated NS protein SC35 (red) and with DAPI dye (blue). α7-CFP fluorescence is in green for easier co-detection (α7-CFP/SC35 image). Wide-field of individual detection and overlay images are presented (63X objective). Bar, 10 μm. (B) 48h induced $U_2$OS-tTA-α7-CFP cells, untreated or treated with DRB (100 $\mu$M) or actinomycin D (10 $\mu$g/ml) for 2 hours before fixation were stained with anti-SC35 (red); α7-CFP expression was directly visualized by CFP fluorescence (cyan) (100X objective). Bar, 10 μm.

**Figure 5.** PA28γ, but not other 20S proteasome regulatory complexes, is recruited together with 20S proteasome into the nuclear foci. (A) 48 hours induced $U_2$OS-tTA-α7-CFP cells were analyzed by indirect immunofluorescence using antibodies directed against the Mss1/Rpt1 and Sug1/Rpt6 ATPase subunits of the 19S complex (red) or PA28β. α7-CFP fusion protein was detected by CFP fluorescence. (B) Subcellular localization of PA28γ (indirect immunofluorescence, red) in parental $U_2$OS-tTA cells and in induced $U_2$OS-tTA-α7-CFP cells. α7-CFP was detected by direct fluorescence. Wide-field of individual areas of detection, overlay images and enlargements of marked area are presented. All observations were done with a 63X objective. Bar, 10 μm.

**Figure 6.** α7 and PA28γ are physically associated in total cell extracts, in a nuclear foci-enriched fraction and *in cellulo*. (A) After lysis of induced $U_2$OS-tTA-α7-CFP cells, the cell extract was clarified by centrifugation and the supernatant was collected (S1). The insoluble material was then resuspended in lysis buffer containing 0.3% Triton-X100 (15 min at 4°C) and clarified by centrifugation, yielding the S2 supernatant. Proteins immunoprecipitated from the S1 and S2 supernatants, using the indicated antibodies, were then separated by SDS-PAGE and analyzed by immunoblotting using antibodies directed against the proteasome subunits α7 (left panel), β2

(right upper panel) or α4 (right lower panel). T: 30 μg of total proteins. (B) The interaction between α7-CFP and PA28γ was visualized *in cellulo* by BiFC. Proteins indicated in each panel were co-expressed in HeLa cells. 24h after transfection of expression vectors, cells were incubated at 32°C for a further 24h to promote chromophore maturation, then fixed to allow YFP fluorescence monitoring. c-Fos (118-210) and c-Jun (257-318) constructs (Hu *et al.*, 2002) were used as positive (Jun-NY/Fos-CY) or negative (Jun-NY/α7-CY and NY-PA28γ/Fos-CY) BiFC controls (63X objective). Bar, 10 μm.

**Figure 7.** Presence of PA28γ in the NS without α7-CFP expression and association of 20S proteasome with SF2/ASF protein. (A) Parental $U_2$OS-tTA cells were permeabilized and fixed simultaneously to remove most of soluble PA28γ complexes. Cells were then stained with anti-SC35 (green) and anti-PA28γ (red) and an overlay image is shown (100X objective). (B) $U_2$OS-tTA cells, co-transfected with pcDNA$_3$-α7 and pEGFP-SF2/ASF vectors, were lysed 24 hours post-transfection in lysis buffer containing 0.3% Triton-X100. 200 μg of total cell extract were subjected to immunoprecipitation using either anti-α4, anti-PA28γ or anti-GFP antibodies. Immunoprecipitated proteins were then separated by SDS-PAGE (10%) and visualized by immunoblotting using anti-GFP antibody. T: 30 μg of total cells extract; S: supernatant of the IP (1/10); IP: immunoprecipitation.

**Figure 8.** Proteasome-PA28γ complexes are required for the integrity of the NS. (A) $U_2$OS-tTA-α7-CFP cells were induced for α7-CFP expression and concomitantly transfected with control-siRNA or PA28γ-siRNA (siRNA#1) duplexes. Cells recovered 48 hours post-transfection, and the expression level of PA28γ was analyzed either by immunoblotting or by indirect immunofluorescence using an anti-PA28γ antibody. Bar, 10 μm. (B) NS were visualized by the fluorescence of α7-CFP and by indirect immunofluorescence using anti-SC35 antibodies in induced $U_2$OS-tTA-α7-CFP cells untransfected or transfected with PA28γ- or control-siRNA duplexes. Enlargements of the marked areas are presented. Bar, 10 μm. (C) Quantification of the number of α7-CFP-labeled NS in cells treated with PA28γ- or control-siRNA duplexes. Quantification was performed visually, by counting on the pictures the number of compact fluorescent foci in each cell. The values correspond to the means of five independent experiments (n = 100 cells, ± SD). (D) 3D reconstruction. SC35 localization was detected by indirect immunofluorescence in induced $U_2$OS-tTA-α7-CFP cells treated with control- or

PA28γ (#1)–siRNA. Fixed cells were observed with a Leica DMRA microscope equipped with a 63X PL APO (NA=1.32) oil immersion objective and a N2.1 (Leica) filter set. Stacks of images were acquired using a piezo stepper (Physik Instruments), Metamorph 7.1 (Molecular Devices) and a Micromax 1300YHS CCD camera (Princeton Instruments). Stacks were further deconvolved using a MLE algorithm and the Huygens 2.9 software (Scientific Volume Imaging) and analyzed in 3D using Imaris 5.3 (Bitplane, Switzerland). (E) NS were visualized by the fluorescence of α7-CFP and by indirect immunofluorescence using anti-SF2/ASF antibodies in induced $U_2$OS-tTA-α7-CFP cells untransfected or transfected with PA28γ- or control-siRNA duplexes. Bar, 10 μm. (F) In parental $U_2$OS-tTA cells, untreated or treated with PA28γ-siRNA duplexes, NS were visualized by indirect immunofluorescence using anti-SC35 antibodies. Bar, 10 μm.

**Figure 9.** Specificity of the effect of the siRNA directed against PA28γ. $U_2$OS-tTA cells were treated or not with PA28γ-siRNA duplexes (# 2), PA28γ-siRNA duplexes (# 2) and pcDNA$_3$-3HA-PA28γ (allowing the expression of a PA28γ construct refractory to siRNA# 2), and pcDNA$_3$-3HA-PA28γ alone, as indicated. (A) Expression levels of endogenous or exogenous PA28γ was analyzed by immunoblotting using anti-PA28γ or -HA antibodies. (B) Analysis of SC35 and PA28γ localization by indirect immunofluorescence as described in figure 8. Bar, 10 μm.

**Figure 10.** Effect of PA28γ siRNA on subnuclear domains. Localization of proteins marker of Cajal (A) and PML Bodies (B) was analyzed in induced $U_2$OS-tTA-α7-CFP cells treated with control- or PA28γ-siRNA, as described in Figure 8. Cells were stained with antibodies raised against three components of CB: TGS1, SMN and coilin (A), or with antibodies raised against the protein PML (B). Bar, 10 μm.

**Figure 11.** PA28γ-siRNA reduces SF2/ASF accumulation at transcription sites. 2E11 cells were co-transfected with pcDNA$_3$-Tat, pEGFP-SF2/ASF and control- or PA28γ–siRNA (#1) duplexes. After 48 hours, cells were fixed and subjected to *in situ* hybridization using a MS2-Cy3 probe. (A) Right: Merged images of the intracellular distribution of SF2/ASF-GFP (green) and MS2 TS and mRNA (red) under the indicated conditions. Left: magnification of the TS (white square): MS2 detection (red), SF2/ASF-GFP (green), merge (100X objective). Bar, 10 μm. (B) Quantification of the level of SF2/ASF-GFP recruited at the TS. The relative levels of SF2/ASF-

GFP at the TS and at the NS was estimated by quantification of the green fluorescence using the Metamorph software, in cells expressing similar levels of transcripts (estimated by quantification of MS2-Cy3 at TS) and SF2/ASF-GFP in the NS. The values correspond to the means of four independent experiments (n = 40 cells, ± SD). See Figure S3 for illustration of the quantification procedure. (C) PA28γ-siRNA does not affect the level of transcription. Relative mRNA levels for the ribosomal S26 subunit (control) and for the artificial gene in 2E11 cells untreated or treated with the indicated siRNA were analyzed by RT-PCR and agarose gel-electrophoresis.

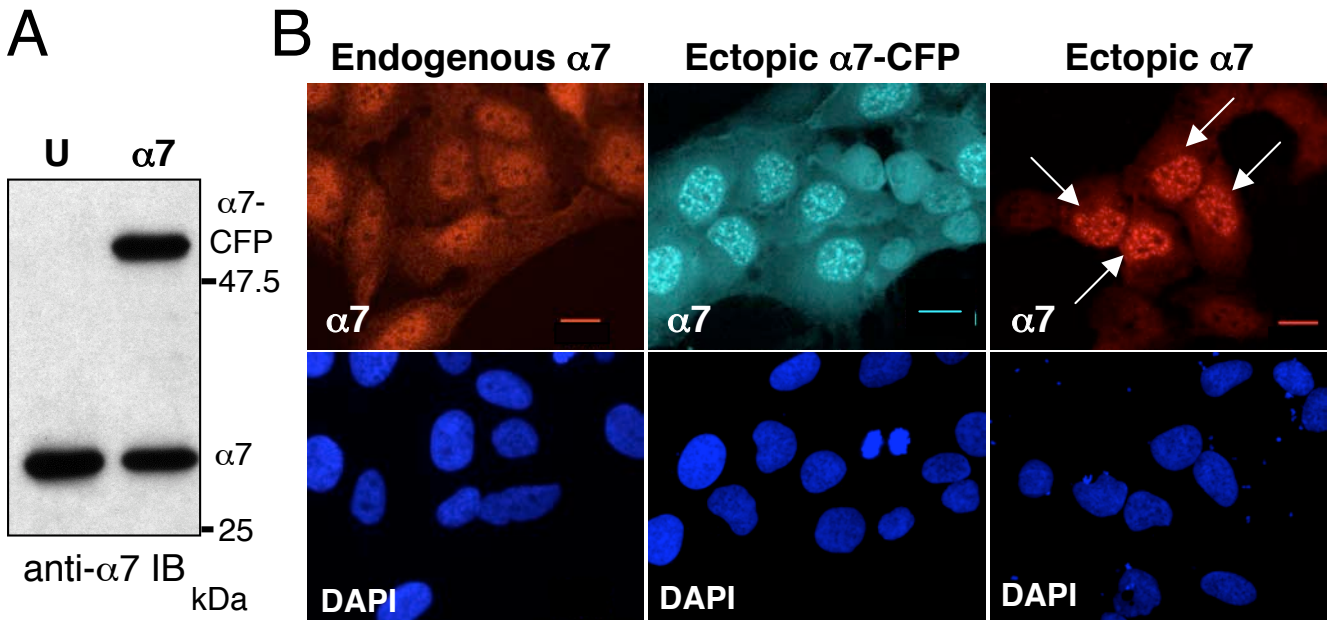
A
U
α7
α7-
CFP
47.5
α7
25
anti-α7 IB
kDa
B
Endogenous α7
Ectopic α7-CFP
Ectopic α7
α7
α7
α7
DAPI
DAPI
DAPI

Figure 1

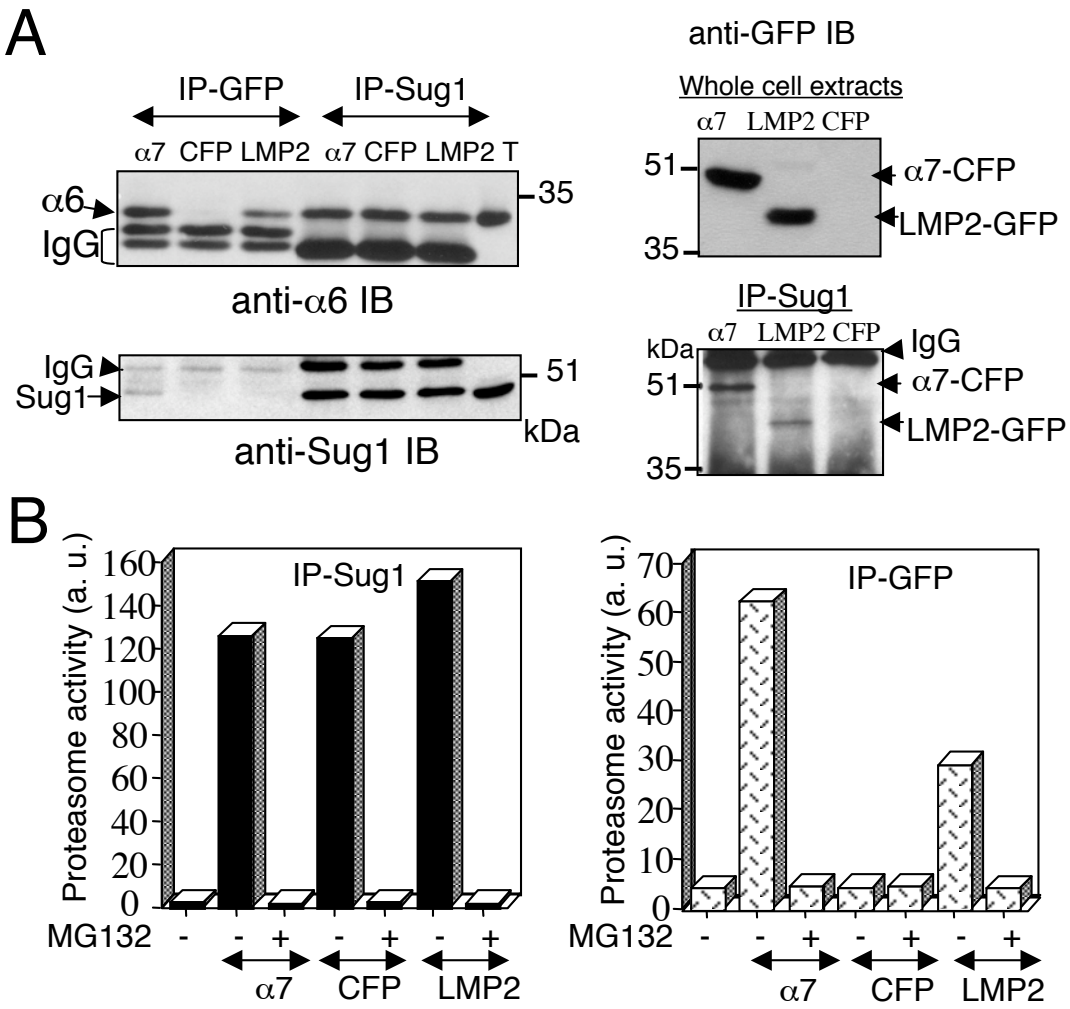
A
IP-GFP
IP-Sug1
α7 CFP LMP2 α7 CFP LMP2 T
α6
IgG
35
anti-α6 IB
IgG
Sug1
51
kDa
anti-Sug1 IB
anti-GFP IB
Whole cell extracts
α7 LMP2 CFP
51
35
α7-CFP
LMP2-GFP
IP-Sug1
α7 LMP2 CFP
kDa
51
35
IgG
α7-CFP
LMP2-GFP
B
Proteasome activity (a. u.)
IP-Sug1
160
140
120
100
80
60
40
20
0
MG132 - - + - + - +
α7 CFP LMP2
Proteasome activity (a. u.)
IP-GFP
70
60
50
40
30
20
10
0
MG132 - - + - + - +
α7 CFP LMP2

Figure 2

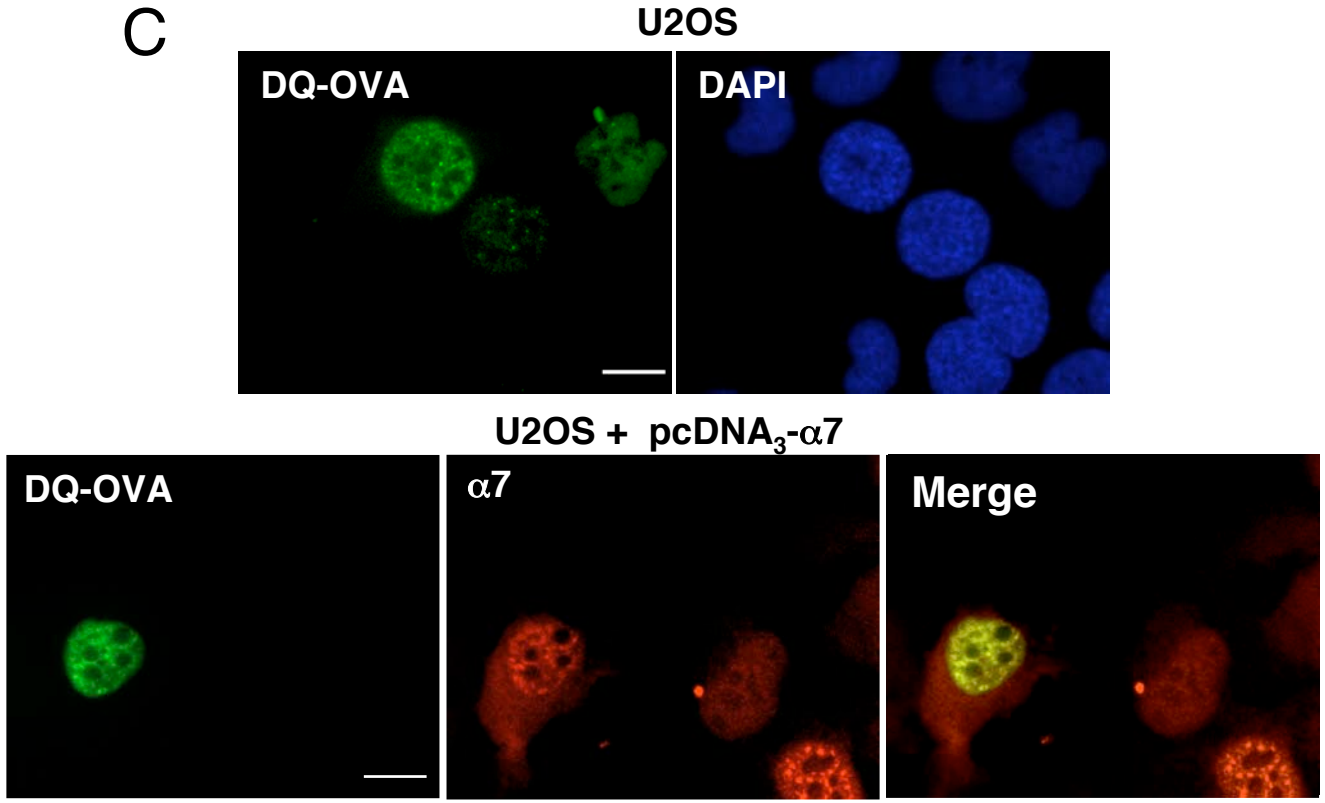


Figure 2

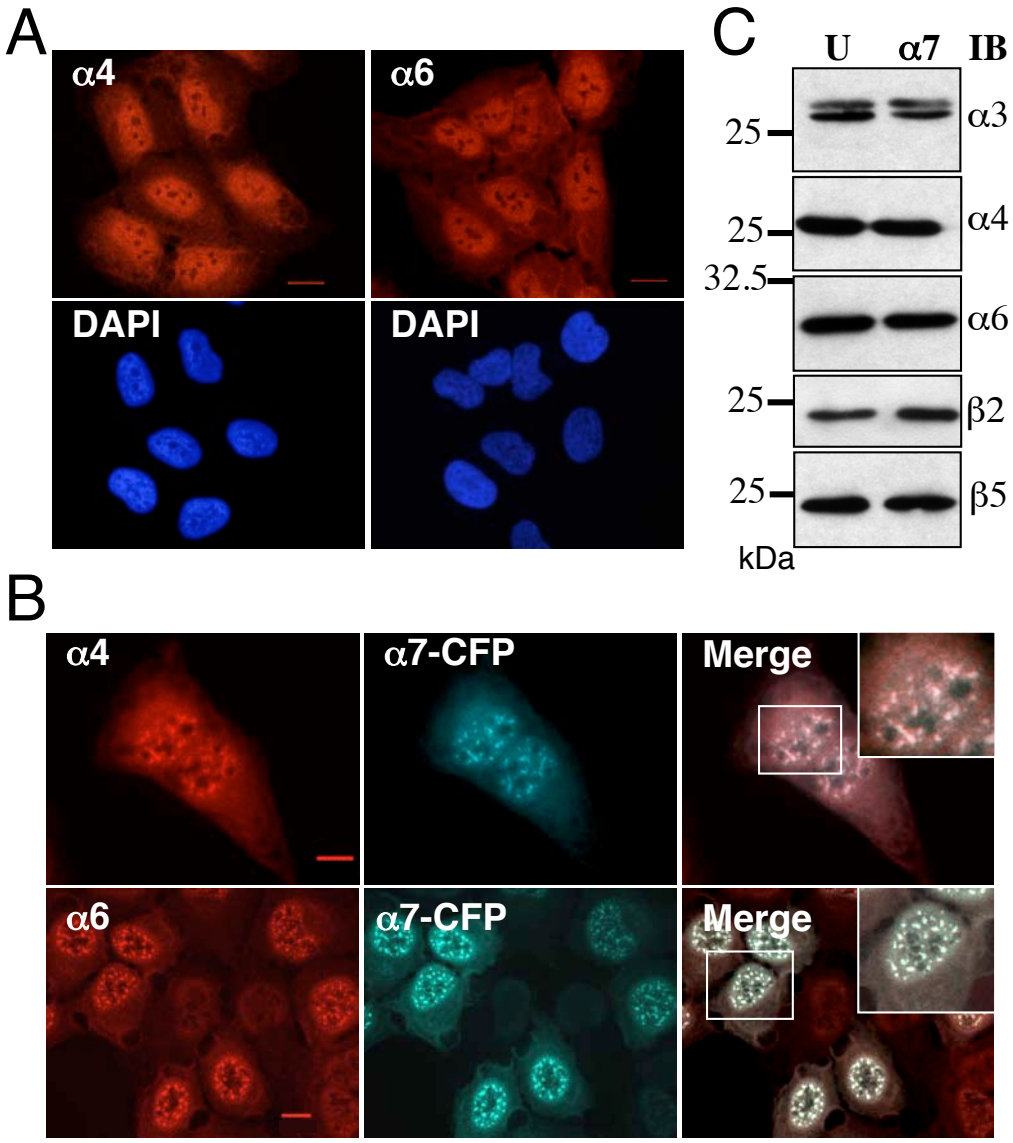
A
α4
α6
DAPI
DAPI
B
α4
α7-CFP
Merge
α6
α7-CFP
Merge
C
U
α7
IB
25
α3
25
α4
32.5
α6
25
β2
25
β5
kDa

Figure 3

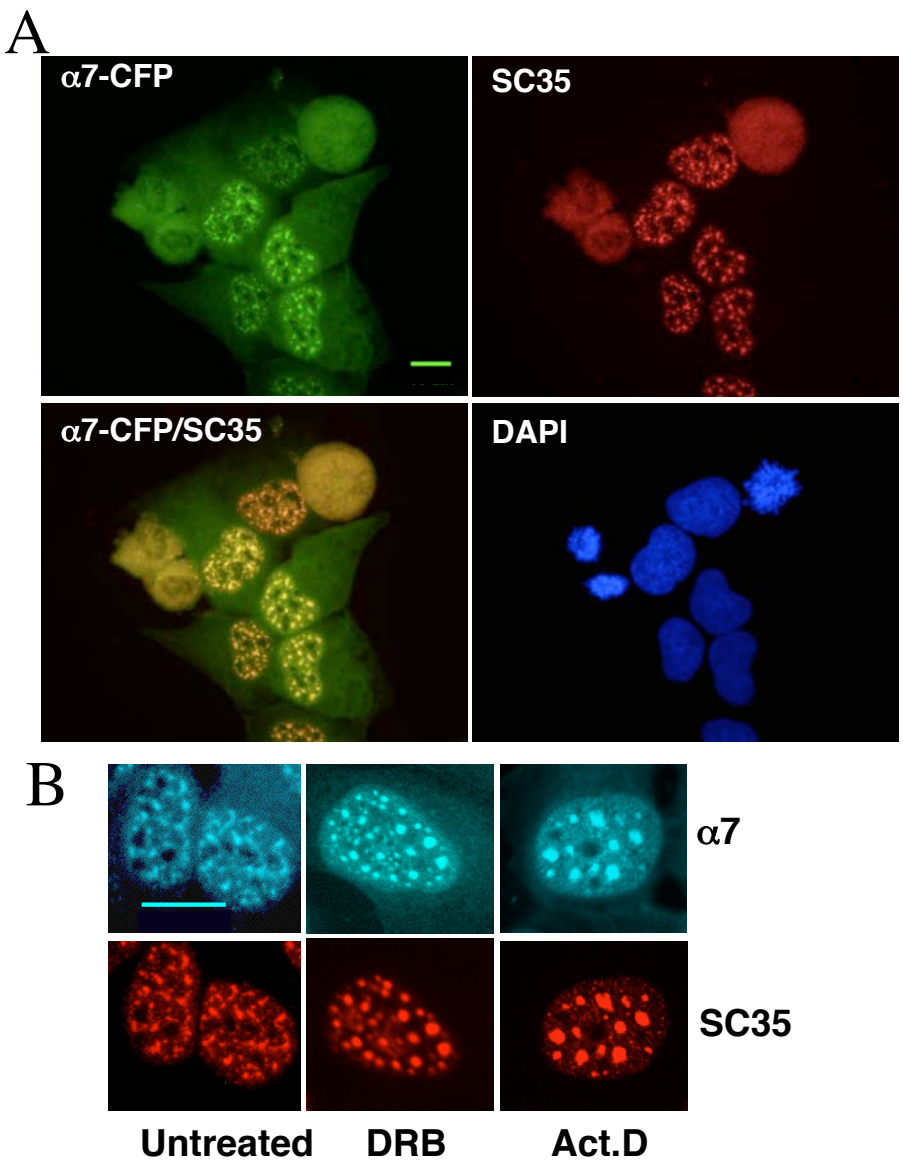


Figure 4

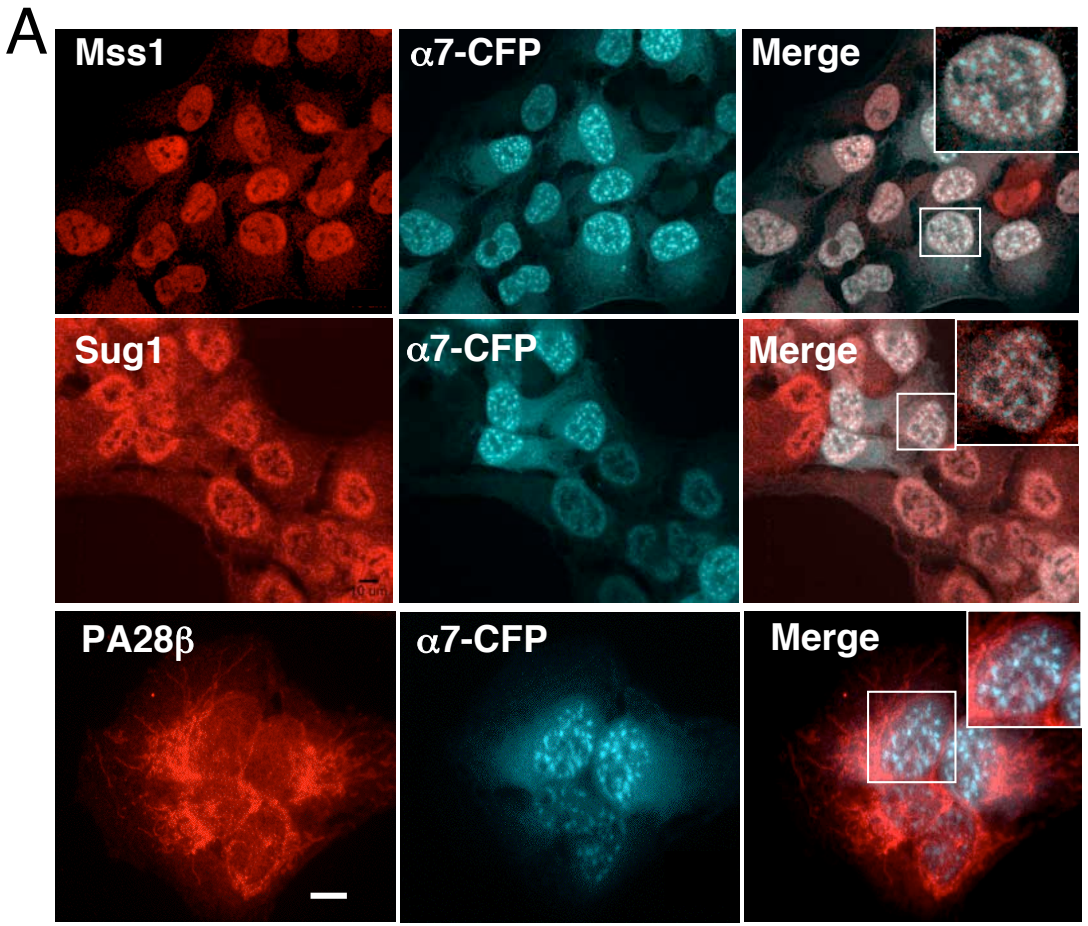


Figure 5

B

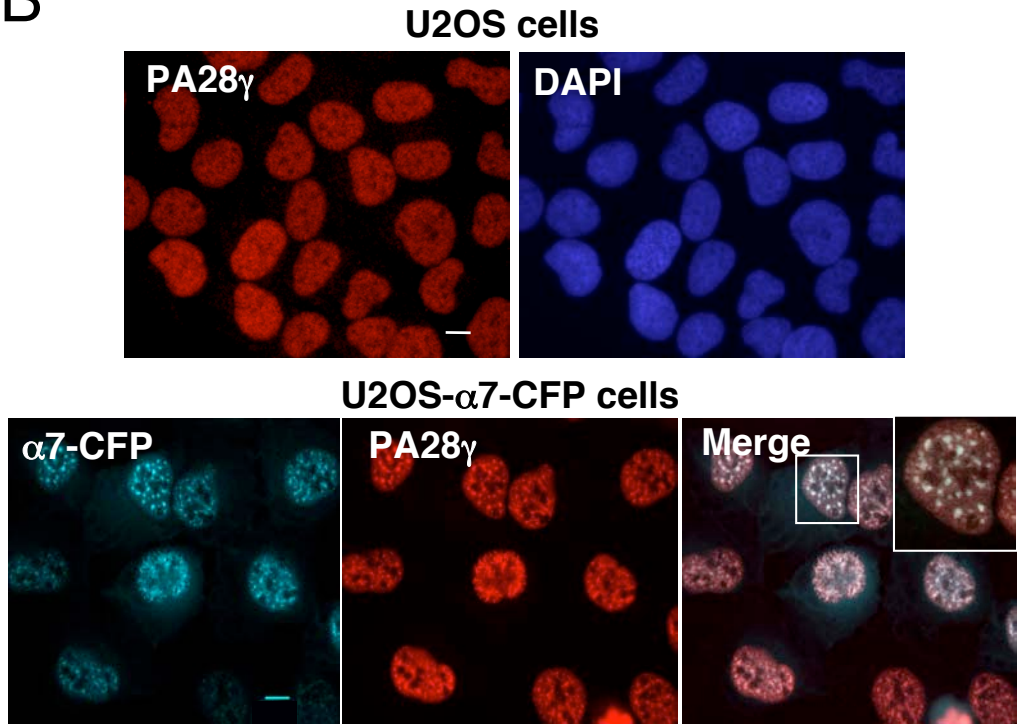


Figure 5

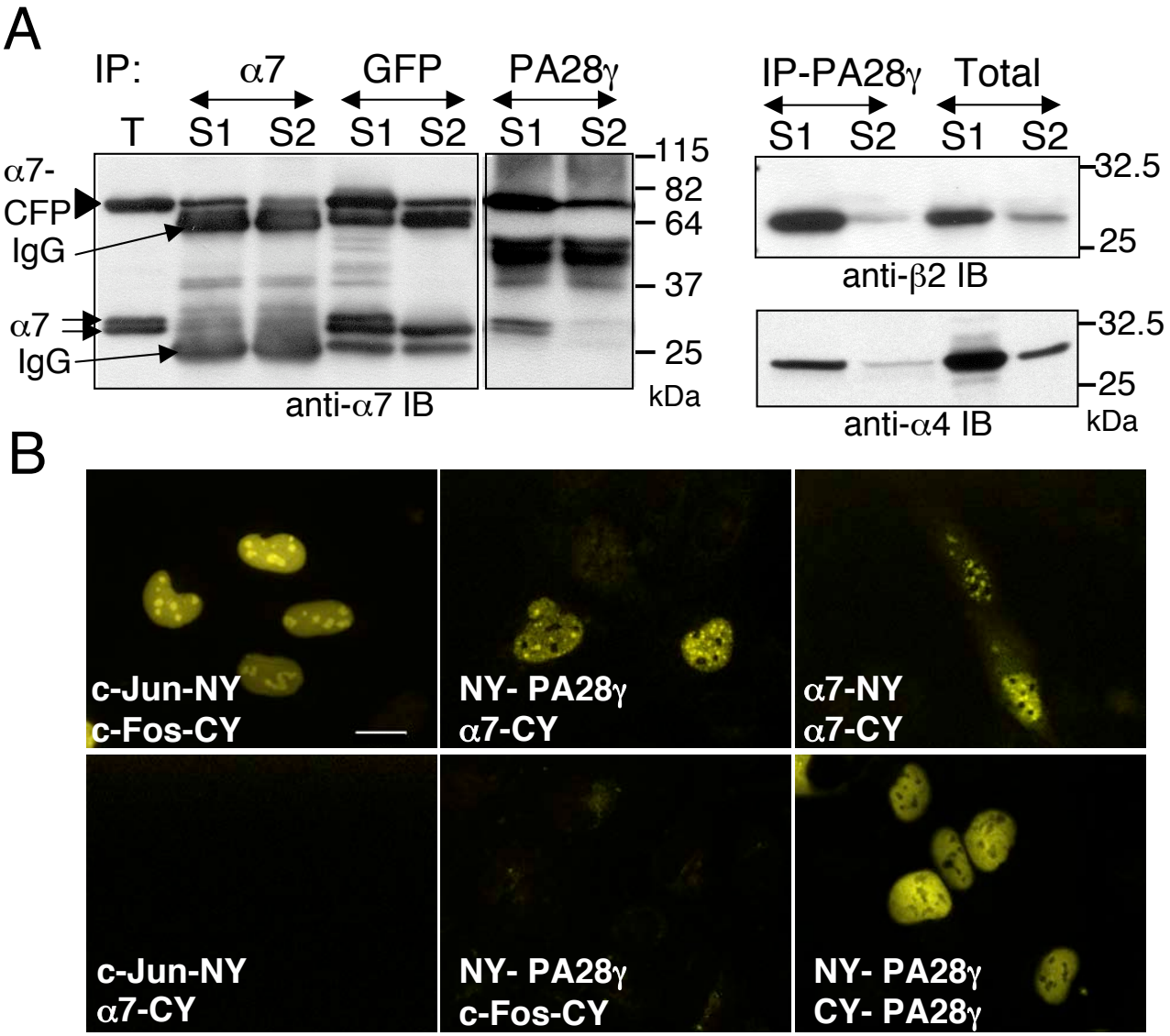
A
IP:
α7
GFP
PA28γ
T
S1
S2
S1
S2
S1
S2
α7-
CFP
IgG
α7
IgG
115
82
64
37
25
kDa
anti-α7 IB
IP-PA28γ
Total
S1
S2
S1
S2
32.5
25
anti-β2 IB
32.5
25
kDa
anti-α4 IB
B
c-Jun-NY
c-Fos-CY
NY- PA28γ
α7-CY
α7-NY
α7-CY
c-Jun-NY
α7-CY
NY- PA28γ
c-Fos-CY
NY- PA28γ
CY- PA28γ

Figure 6

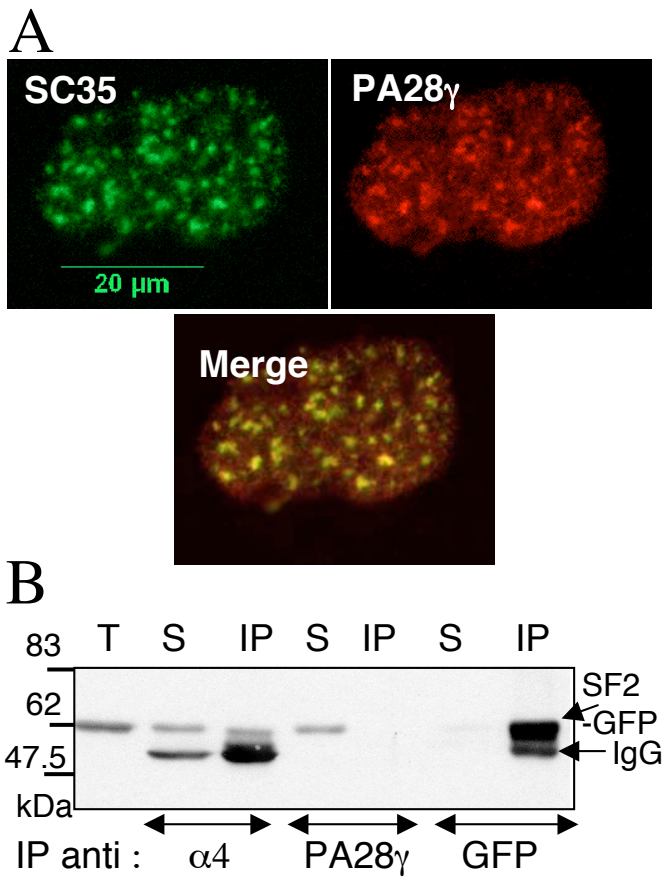
A
SC35
PA28γ
20 µm
Merge
B
83
62
47.5
kDa
T
S
IP
S
IP
S
IP
SF2
-GFP
IgG
IP anti :
α4
PA28γ
GFP

Figure 7

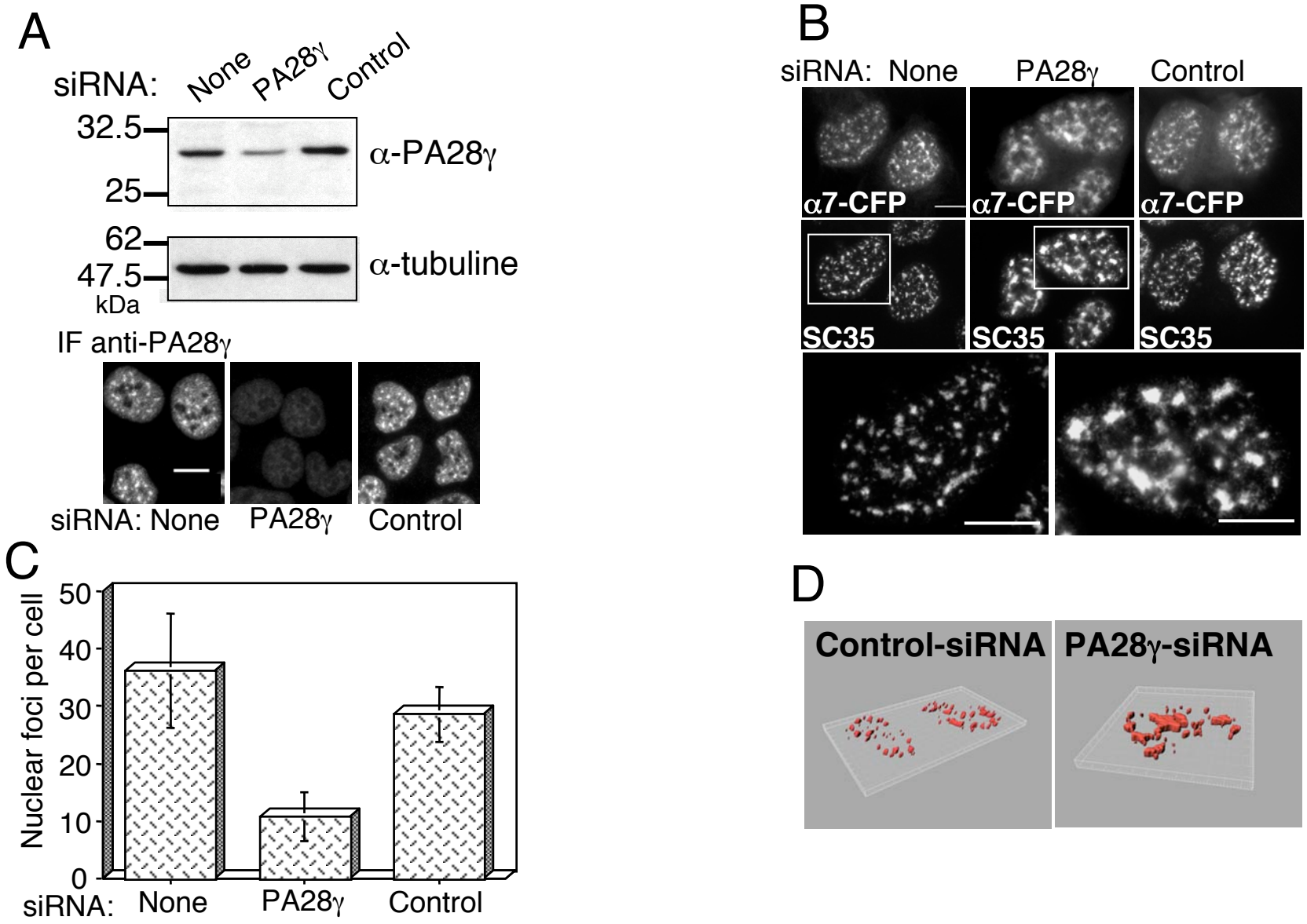
A
siRNA: None PA28γ Control
32.5
25
α-PA28γ
62
47.5
kDa
α-tubuline
IF anti-PA28γ
siRNA: None PA28γ Control
B
siRNA: None PA28γ Control
α7-CFP
α7-CFP
α7-CFP
SC35
SC35
SC35
C
Nuclear foci per cell
50
40
30
20
10
0
siRNA: None PA28γ Control
D
Control-siRNA
PA28γ-siRNA

Figure 8

E

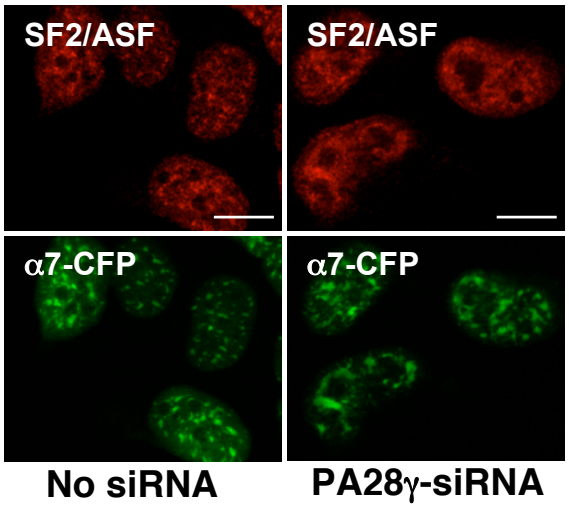
SF2/ASF
SF2/ASF
α7-CFP
α7-CFP
No siRNA
PA28γ-siRNA

F

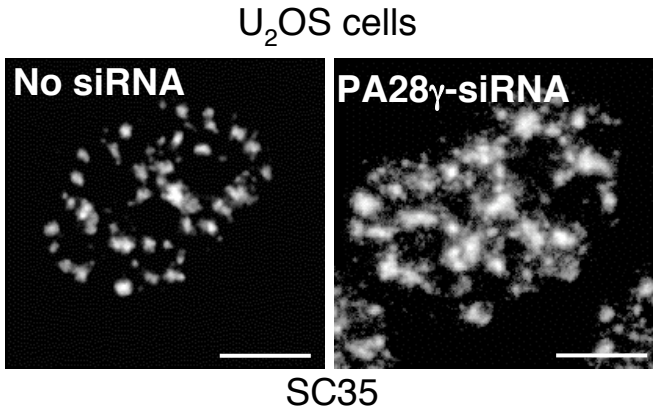
U2OS cells
No siRNA
PA28γ-siRNA
SC35

Figure 8

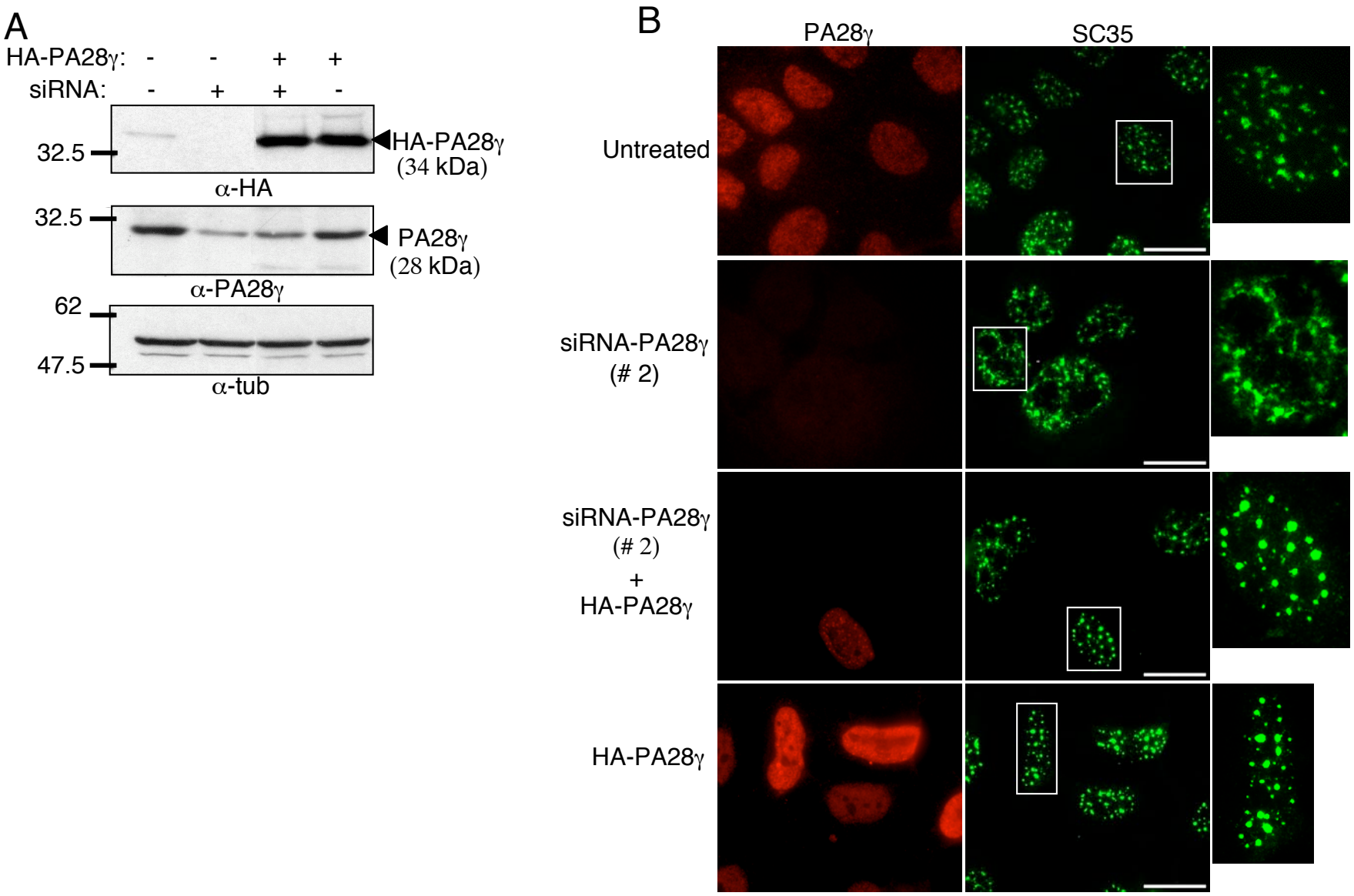
A
HA-PA28γ: - - + +
siRNA: - + + -
32.5
HA-PA28γ
(34 kDa)
α-HA
32.5
PA28γ
(28 kDa)
α-PA28γ
62
47.5
α-tub
B
PA28γ
SC35
Untreated
siRNA-PA28γ
(# 2)
siRNA-PA28γ
(# 2)
+
HA-PA28γ
HA-PA28γ

Figure 9

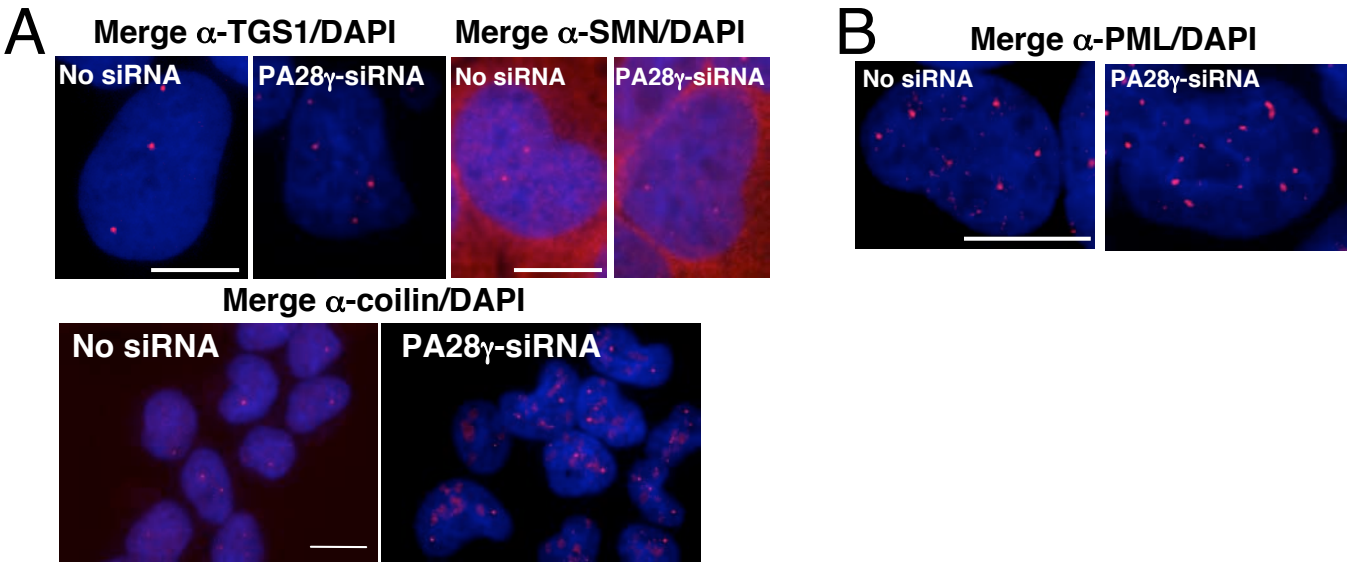
A
Merge α-TGS1/DAPI
Merge α-SMN/DAPI
No siRNA
PA28γ-siRNA
No siRNA
PA28γ-siRNA
Merge α-coilin/DAPI
No siRNA
PA28γ-siRNA
B
Merge α-PML/DAPI
No siRNA
PA28γ-siRNA

Figure10

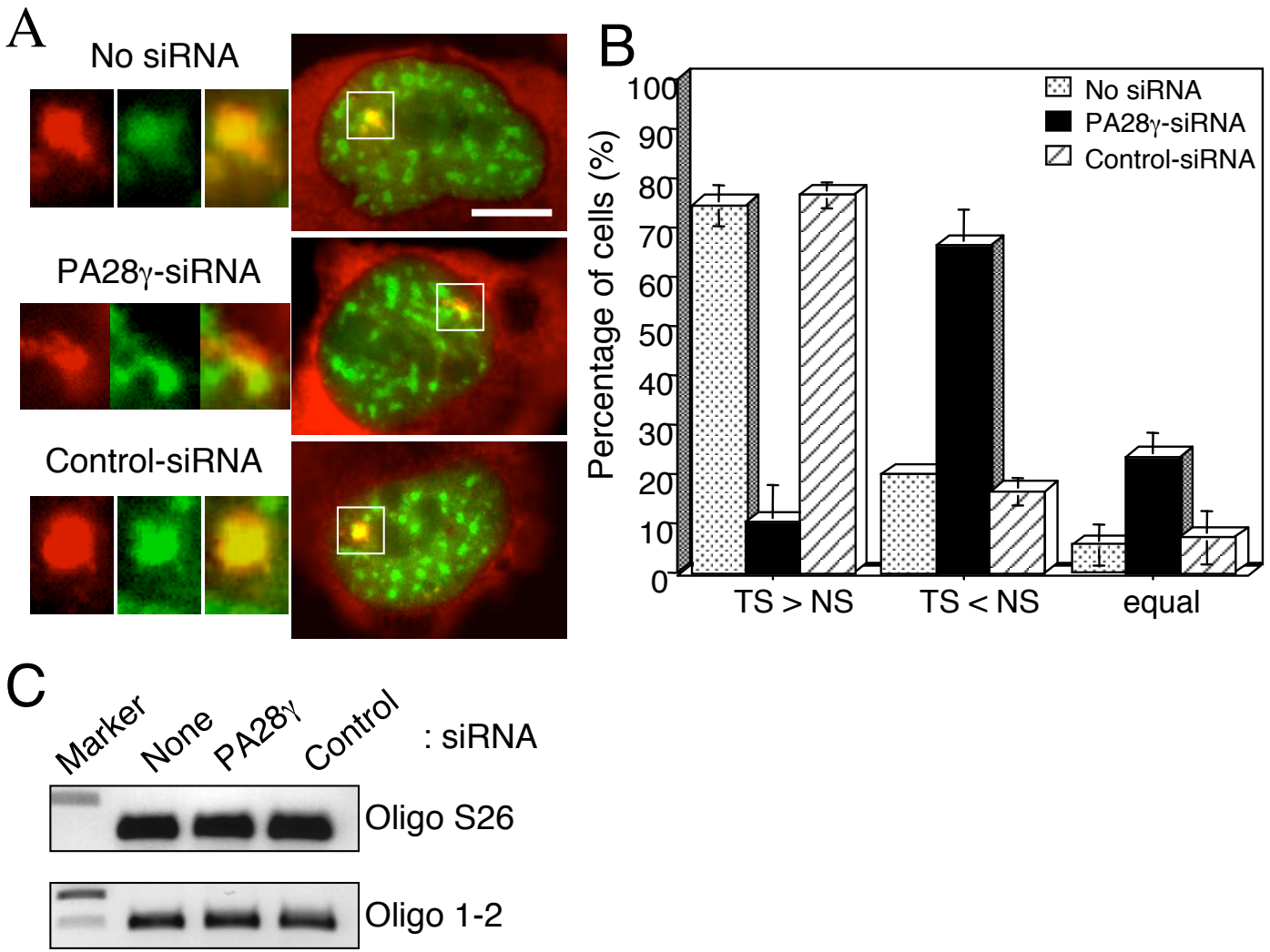
A
No siRNA
PA28γ-siRNA
Control-siRNA
B
Percentage of cells (%)
100
90
80
70
60
50
40
30
20
10
0
No siRNA
PA28γ-siRNA
Control-siRNA
TS > NS
TS < NS
equal
C
Marker
None
PA28γ
Control
: siRNA
Oligo S26
Oligo 1-2

Figure 11

**Legends for supplemental material**

**Figure S1.** Cellular distribution of α7-CFP, 20S proteasome and PA28γ during mitosis. α7-CFP, α6 or PA28γ were detected by fluorescence (α7-CFP) or indirect immunofluorescence (α6 and PA28γ) in $U_2$OS-tTA-α7-CFP cells induced for 48h and at different stages of mitosis.

**Figure S2.** (A) Confocal microscopy analyses of the localization of α4, Mss1, Sug1, PA28γ (indirect immunofluorescence) and α7-CFP (direct detection) in induced $U_2$OS-tTA-α7-CFP cells. A confocal scanning laser microscope (Zeiss LSM Meta 510) was used. Bar, 10 μm. (B) Fluorescence analysis of images shown in figures 3B, 5A-B. NS levels of α7-CFP (direct fluorescence), α4, Mss1, Sug1 and PA28γ (indirect immunofluorescence) were quantified using the "line scan" function of Metamorph software. Left: Images show merge pictures of nuclear α7-CFP (green) and α4, Mss1, Sug1 and PA28γ respectively (red). The scanned line is indicated. Right: line scan results: intensities of green and red signals along the line were measured and plotted.

**Figure S3.** Quantification of the GFP and MS2-Cyan3 fluorescence. Fluorescence levels of SF2/ASF-GFP protein and MS2-Cy3 probe in cells treated with PA28γ-siRNA or control-siRNA, or untreated cells, were quantified using the line-scan measure of the Metamorph software. Left: images show a merge picture of SF2/ASF-GFP distribution (green) and MS2 mRNA (red). Right: a line (white) crossing both the transcription site (TS) and a NS was drawn and the intensity of both red and green signals along the line were measured and plotted. The recruitment, or not, of SF2/ASF-GFP at TS was estimated by comparing its level at TS to its level in NS. Data were collected using cells showing the same level of transcription, determined by MS2-Cy3 fluorescence.

**Figure S4.** Knockdown of PA28γ has no global effect on transcription or pre-mRNA splicing. (A) The level of transcription was not affected specifically by PA28γ siRNA. Nuclei were labelled with 5-FU (2 mM, 40 min.) to monitor ongoing transcription in $U_2$OS-tTA-α7-CFP induced cells untreated (none) or treated with control- or PA28γ-siRNA, as in Figure 7. Incorporated 5-FU was detected using an anti-BrdU antibody and the fluorescence was quantified using the Metamorph software on several independent fields. The values correspond to the means of four independent experiments (n = 60 cells, ± SD). Note that the unspecific increase of transcription could be related to the data of Semizarov *et al.*[(1)], which showed by microarray

analysis that siRNA cause a non-specific 4- to 8-fold induction of a large number of common genes. (B) Splicing of endogenous genes was not affected by siRNA treatment. $U_2$OS-tTA-α7-CFP cells were either untreated (none) or treated for 72 hr with PA28γ or control siRNA. After purification of total RNA, RT-PCR analysis of the Clk/Sty, CD44, SC35, and Bcl-X mRNA species was performed. Briefly, first-strand cDNA was synthesized from 5μg of total RNA with the Amersham cDNA synthesis kit. *SC35*, *Clk*/*Sty*, *CD44*, and *Bcl-X* alternatively spliced mRNA isoforms were amplified with Taq polymerase (Invitrogen) with the following forward (f) and reverse (r) primers (name; sequence is given 5' to 3'): *SC35* (f), CAAGTCTCCTGAAGAGGAAGG; *SC35* (r), GTTCCAAGGACTCTTCTTCG; *Clk*/*Sty* (f), GCATAGTAGCAAGTCCTCTG; *Cly*/*Sty* (r), TACTGCTACACGTCTACCTC; *CD44* (f), CTATTGTCAACCGTGATGGTAC; *CD44* (r), GCCAGGAGAGATGCCAAGATG; *Bcl-X* (f), ATGTCTCAGAGCAACCGGGA; *Bcl-X* (r), TCACTTCCGACTGAAGAGTG. Alternative splicing patterns reported for the primary transcripts are depicted on the right. Alternative exons are indicated by black dotted boxes. The positions of primers and expected sizes (in nucleotides, nt) of the RT-PCR products corresponding to the different mRNA isoforms are indicated. Correspondences between RT-PCR products and mRNA isoforms are shown on the right of the gels. The position of the size markers (in base pairs, bp) are indicated on the left. The GAPDH RT-PCR control used to normalize for RNA amounts is also presented. (C) PA28γ siRNA did not affect alternative splicing of PDH construct. $U_2$OS-tTA-α7-CFP cells were transiently transfected with βm3S1-PDH (1, 2, 3) or βm3S1-PDHmut (4, 5, 6) (these two constructs were previously described in Gabut *et al* [(2)]). Cells were either untreated (none) or treated for 72 hr with PA28γ or control siRNA. Total RNA purified from the transfected cells was analysed by RT-PCR. RNA amount was normalized by Neomycine RT-PCR.

[(1)] *Semizarov et al.* (2003) PNAS, 100, 6347-6352. [(2)] Gabut M. *et al.* (2005) Mol Cell Biol., 8, 3286-3294.

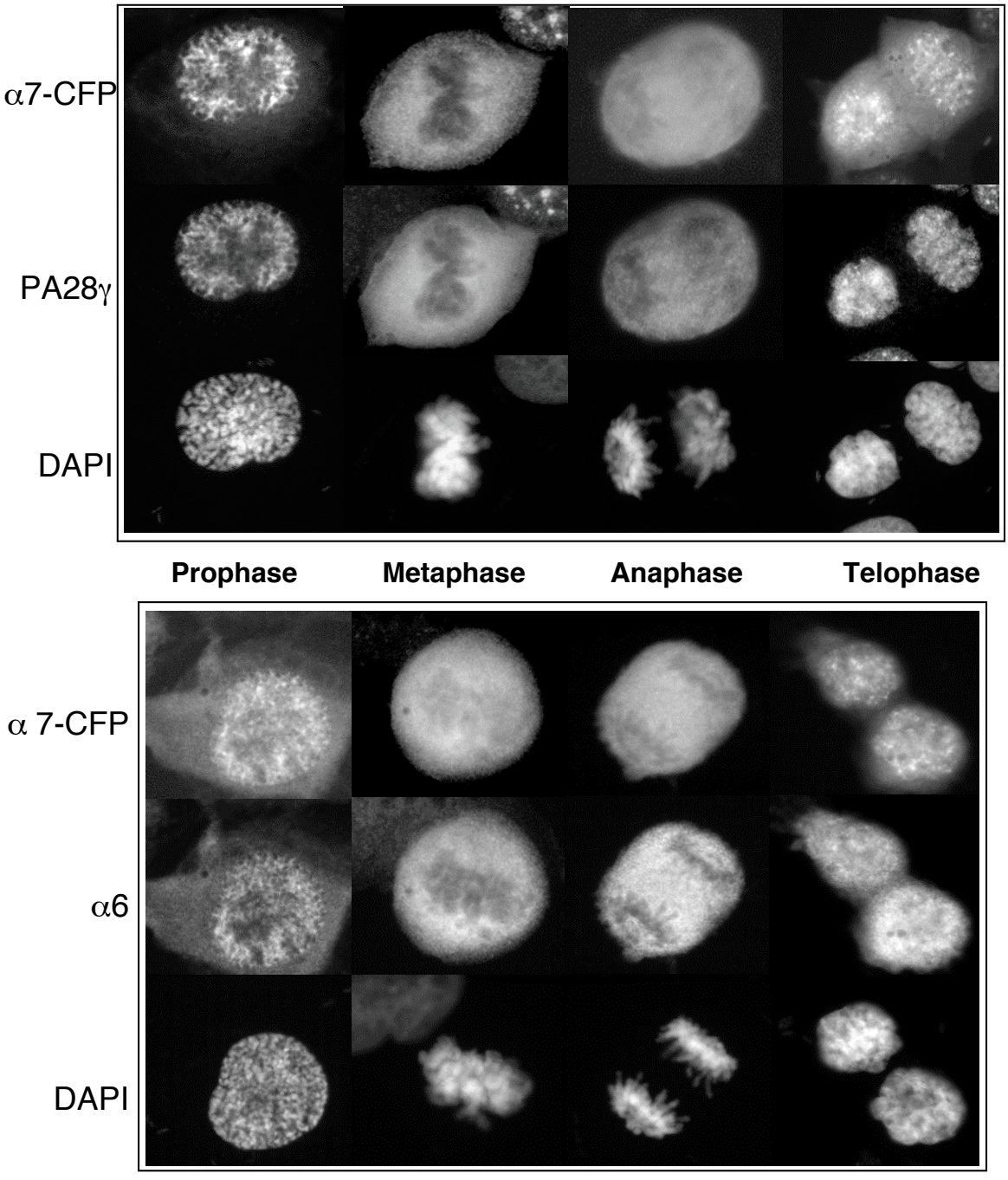
α7-CFP
PA28γ
DAPI
Prophase
Metaphase
Anaphase
Telophase
α 7-CFP
α6
DAPI

**Figure S1**

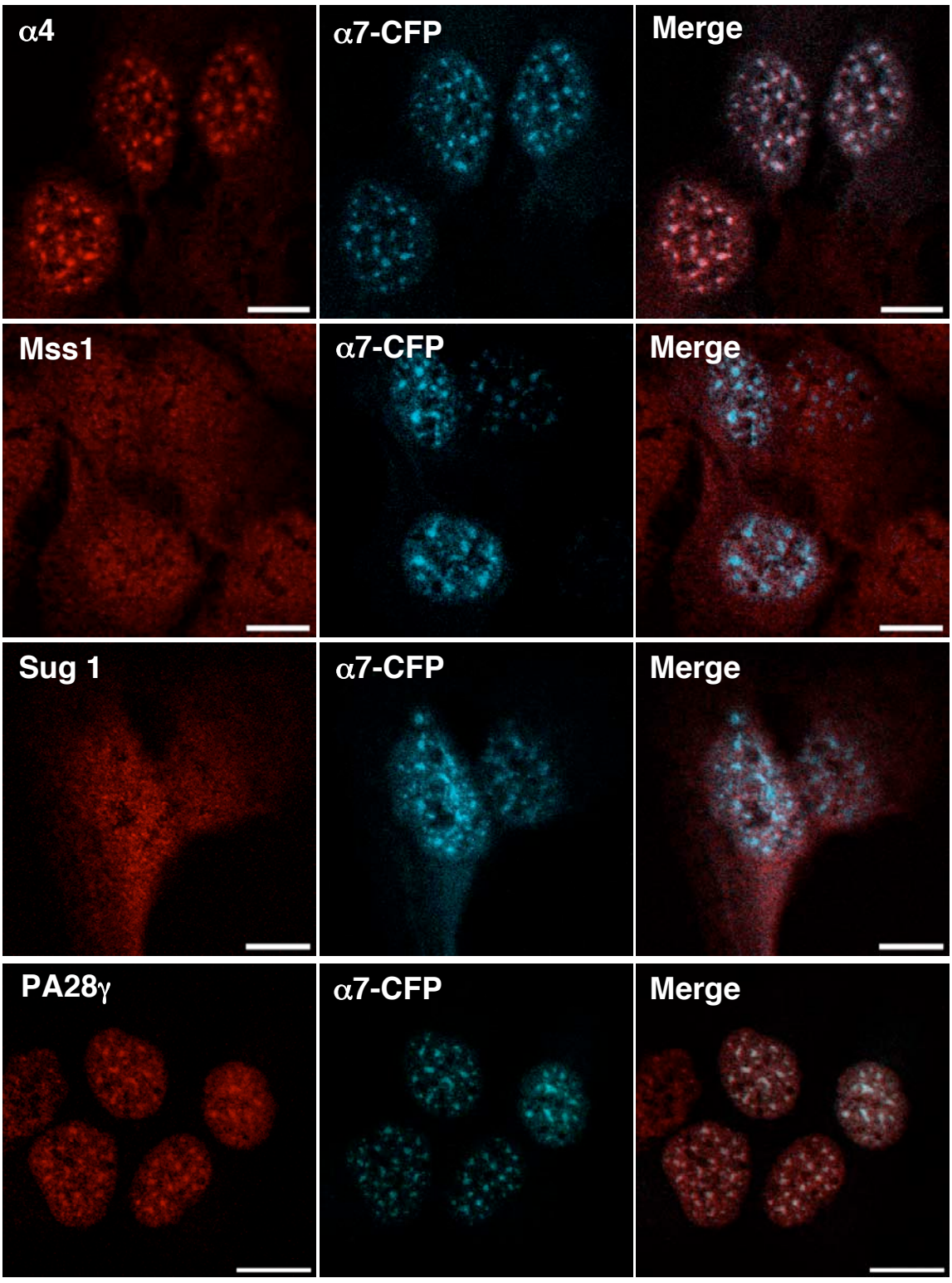
α4
α7-CFP
Merge
Mss1
α7-CFP
Merge
Sug 1
α7-CFP
Merge
PA28γ
α7-CFP
Merge

**Figure S2A**

α4/α7-CFP (merge)

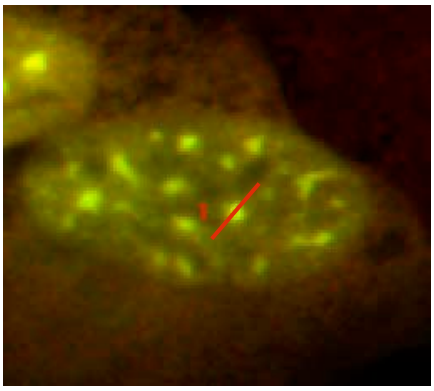


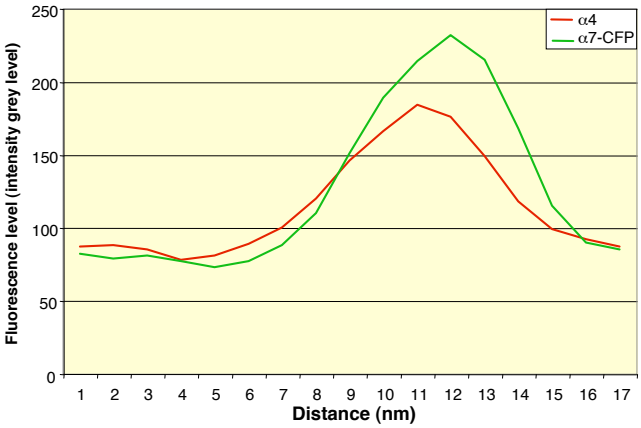


Mss1/ α7-CFP (merge)

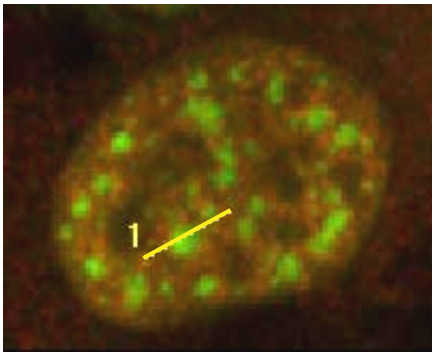


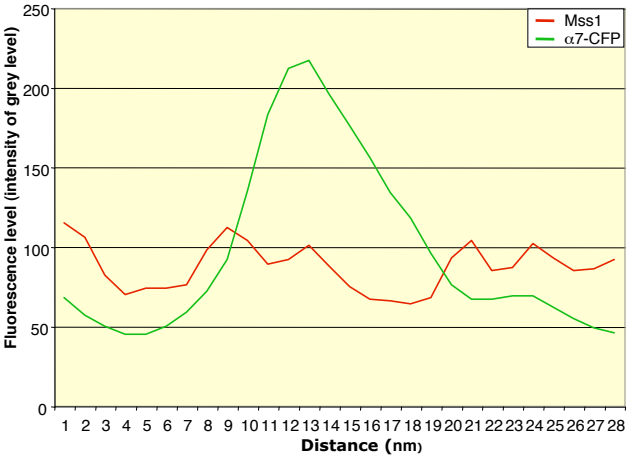


Sug1/ α7-CFP (merge)

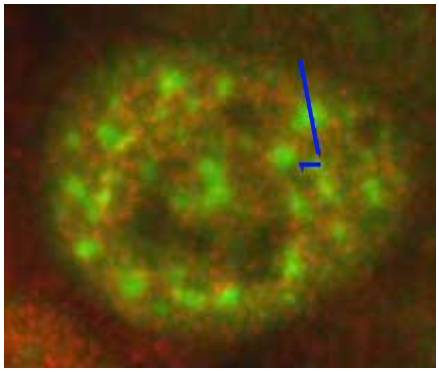


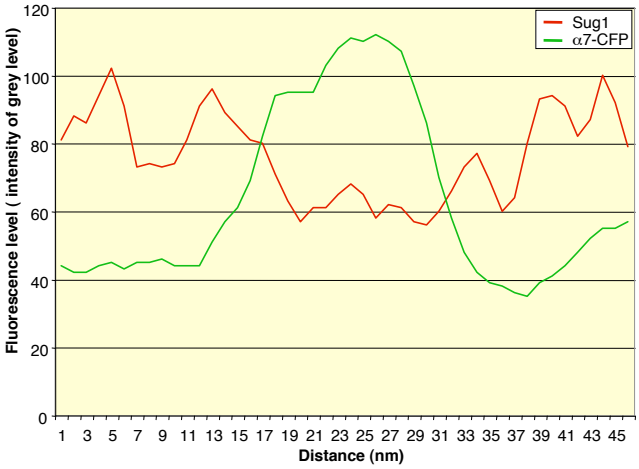


PA28γ/ α7-CFP (merge)

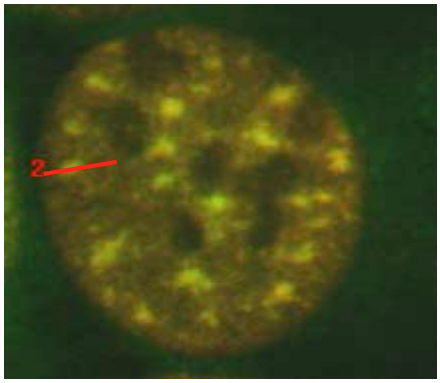


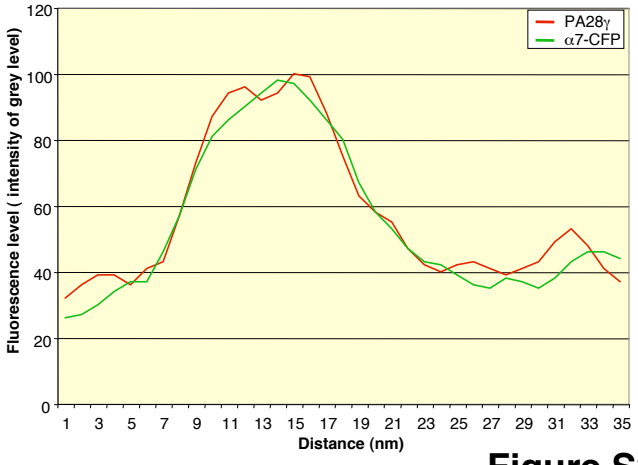


**Figure S2B**

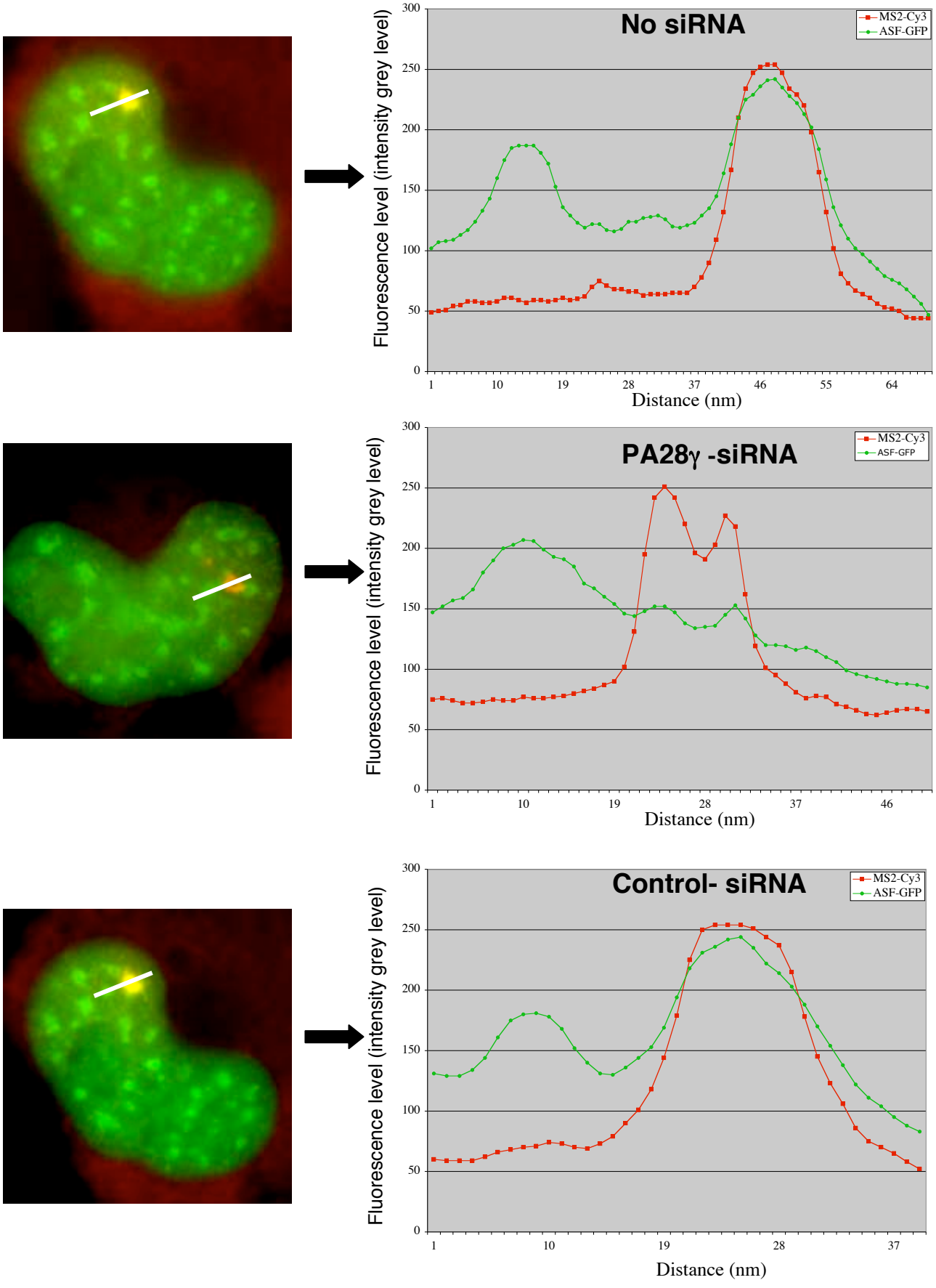
No siRNA
MS2-Cy3
ASF-GFP
Fluorescence level (intensity grey level)
Distance (nm)
PA28γ -siRNA
MS2-Cy3
ASF-GFP
Fluorescence level (intensity grey level)
Distance (nm)
Control- siRNA
MS2-Cy3
ASF-GFP
Fluorescence level (intensity grey level)
Distance (nm)

**Figure S3**

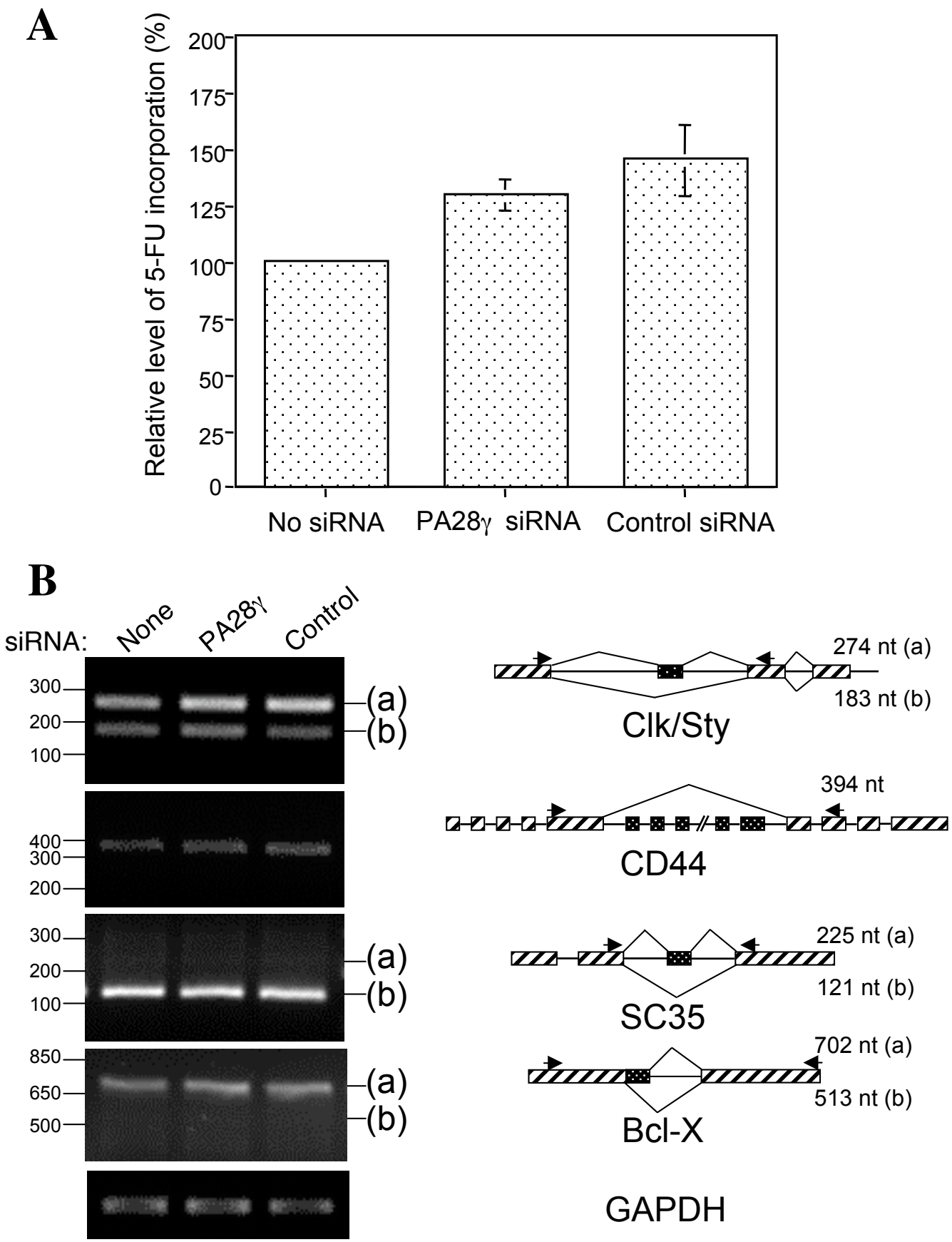
A
Relative level of 5-FU incorporation (%)
200
175
150
125
100
75
50
25
0
No siRNA
PA28γ siRNA
Control siRNA
B
siRNA:
None
PA28γ
Control
300
200
100
(a)
(b)
400
300
200
300
200
100
(a)
(b)
850
650
500
(a)
(b)
274 nt (a)
183 nt (b)
Clk/Sty
394 nt
CD44
225 nt (a)
121 nt (b)
SC35
702 nt (a)
513 nt (b)
Bcl-X
GAPDH

**Figure S4**

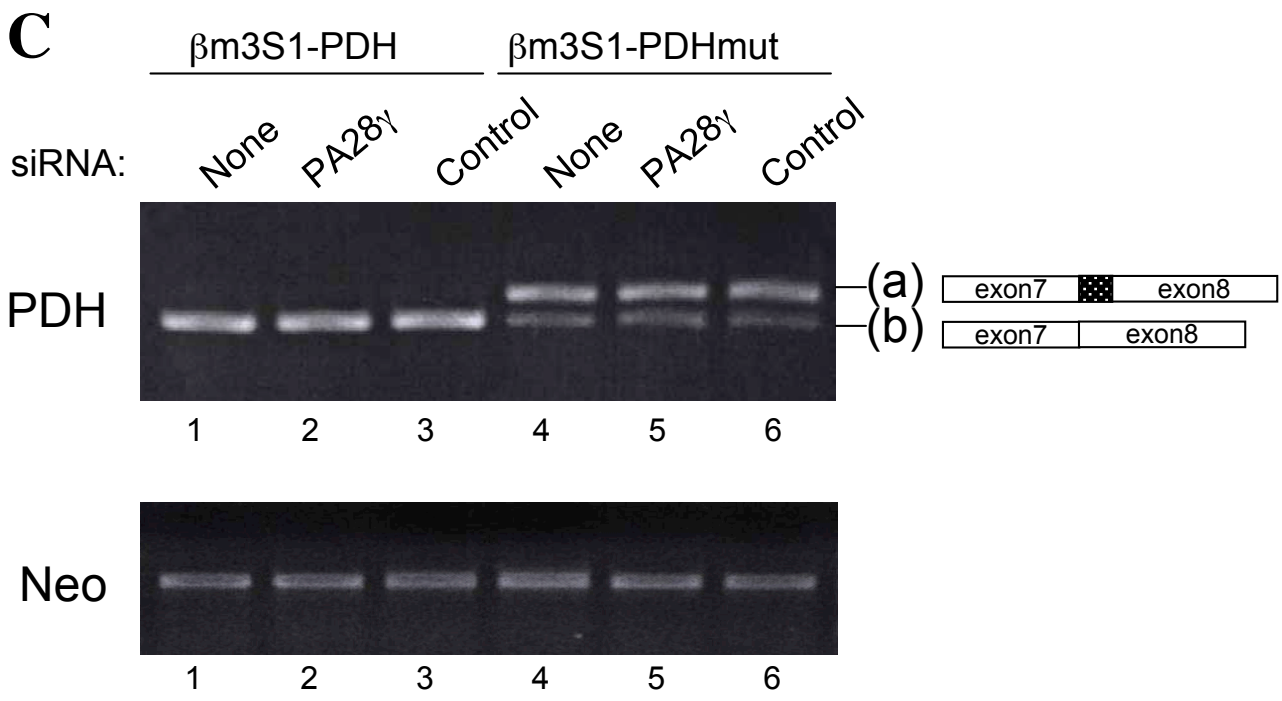
C
βm3S1-PDH
βm3S1-PDHmut
siRNA:
None
PA28γ
Control
None
PA28γ
Control
PDH
(a)
(b)
exon7
exon8
exon7
exon8
1 2 3 4 5 6
Neo
1 2 3 4 5 6

**FigureS4**